

On interdependence among transmit and consumed power of macro base station technologies

Josip Lorincz, Toncica Matijevic and Goran Petrovic

FESB, University of Split
R. Boskovicica 32, 21000 Split, Croatia
[e-mail: josip.lerinc@fesb.hr]
[e-mail: toncica.matijevic@fesb.hr]
[e-mail: goran.petrovic@fesb.hr]

*Corresponding author: Josip Lorincz

E-mail of corresponding author: josip.lerinc@fesb.hr

Address of corresponding author: FESB, University of Split, R. Boskovicica 32, 21000 Split, Croatia

Contact phone of corresponding author: +385 91 4 305 665

Abstract – Dynamic adaptation of the base stations on/off activity or transmit power, according to space and time traffic variations, are measures accepted in the most contemporary resource management approaches dedicated to improving energy efficiency of cellular access networks. Practical implementation of both measures results in changes to instantaneous base station power consumption. In this paper, extensive analyses presenting influence of the transmit power scaling and on/off switching on instantaneous macro base stations power consumption are given. Based on real on-site measurements performed on a set of macro base stations of different access technologies and production years, we developed linear power consumption models. These models are developed by means of linear regression and precisely model the influence of transmit power on instantaneous power consumption for the second, third and fourth generations of macro base stations. In order to estimate the potential energy savings of transmit power scaling and on/off switching for base stations of different generations, statistical analyses of measured power consumptions are performed. Also, transient times and variations of base stations instantaneous power consumption during transient periods initiated with on/off switching and transmit power scaling are presented. Since the developed power consumption models have huge confidence follow measured results, they can be used as general models for expressing the relationship between transmitted and consumed power for macro base stations of different technologies and generations.

Keywords – modeling, power, base station, green, wireless, measurements, consumption, transmit, energy

1. Introduction

Telecommunication systems have experienced enormous growth over the last decade. In order to satisfy subscriber demand, broadband service providers and telecommunication network operators are expected to extend their networks. In such a manner, they will not only increase the size, complexity and density of the network, but also associated energy consumption which, due to economic and environmental reasons, becomes an important issue.

Nowadays, the information and communication technologies (ICT) sector is responsible for about 3 percent of the world's power consumption and 2 percent of closely related carbon emissions [1], [2]. The amount of carbon emission depends on technology used for energy production. In the case of the ICT sector, approximately 500g CO₂e/kWh is emitted [3]. This number is even higher for the case of off-grid base stations (BSs) that are powered by diesel generators. Such BS sites consume, for example, 4.8 kW and spew into the atmosphere 33.3 tons of CO₂ annually [4]. Another key driver for reducing energy consumption is frequently rising energy prices. For example, in a European operator cellular network around 18 percent of operational expenditures (OPEX) are expenses related to energy costs. These costs are even higher for operators in developing countries [5] that have a significant percentage of diesel-powered BS sites.

Cellular telecommunication systems contribute to a large fraction of the total energy consumed by the ICT sector. Thus, a reduction of cellular networks' power consumption will noticeably contribute to an overall power consumption reduction of the whole ICT sector. The major part of energy is consumed in the radio

access part of cellular networks, more precisely the BSs. BSs contribute approximately between 60 and 80 percent of total cellular network energy consumption [6]. The reason behind such a significant portion in overall power consumption is the large number of BSs deployed in the network. Due to subscribers' demands for high data speeds reachable in any part of an operator's network, in parallel with legacy BSs of the 2nd and 3rd generations (2G and 3G), operators introduced 4th generation (4G) technology which is expecting to be even more densely deployed.

Hence, to obtain a discernible reduction of cellular network power consumption, it is necessary to reduce power consumption in the radio part of wireless access networks. The energy-efficient management of network resources, according to space and time variations of traffic, is envisioned as the most promising approach dedicated to the improvement of cellular network energy efficiency. The above mentioned approach takes into account the possibility of dynamically switching on and off all or some parts of the BSs according to traffic pattern variations. Additionally, this is accompanied with adjustment of other radio parameters such as transmit (Tx) power and BSs antenna elevation (tilt). Of huge importance in such an energy-efficient network management scheme is Tx power adaptation, since the level of radiated power directly influences the total power consumption of a BS. For that reason, in this paper we present results obtained through extensive on-site measurements. We perform measurements of the Tx and consumed power for real BSs of different technologies (2G, 3G and 4G) and production periods (from 2000 to 2012). Based on the measured results, the main contribution of this paper is a proposal of the precise models to indicate influence of BSs Tx power on the instantaneous power consumption of BSs.

The rest of the paper is organized as follows. In Section 2, we provide an overview of previous research activities dedicated to the improvement of cellular network energy-efficiency, based on dynamic adaptation of BSs activity or Tx power. Section 3 gives an overview of analyzed BSs technologies with detailed technical specifications of each BS. The measuring setup used for precise measurements of BSs power consumption and theoretical background of linear regression used for modeling interdependence among consumed and transmit power, is presented in Section 4. Measurement results of BS power consumptions for different Tx power levels of each BS technology are discussed in Section 5. In Section 6, the developed linear power consumption models are introduced and commented. Statistics of the BSs power consumption and durations of transient periods initiated with on/off switching and Tx power scaling are presented in Section 7. Finally, a conclusion and plans for future research activities are given in Section 8.

2. Related work

Over the last few years there have been a considerable amount of research activities dealing with energy efficiency of cellular radio access networks. In this section, we present a brief overview of the studies in which the Tx power of BS is taken as parameter that affects network energy efficiency.

For estimating the energy efficiency of a complete cellular network, a few metrics defined in [7] are commonly used. Each of these takes network power consumption as parameter, for calculation of which, realistic BS power consumption model has great importance. These models indicate how total BS power consumption depends on Tx power. Generally, few different models in which Tx power is taken as parameter are proposed in the literature. According to the model proposed in [8], total BS power consumption is determined as the sum of powers consumed by individual BS components. In this model, consumption of the power amplifier (PA) is the most significant since it is the Tx power dependent component with a share of around 65 percent of total BS power consumption [9].

In article [10], it is assumed that power consumption of a macro BS is load independent. Thus a linear power consumption model of simple form, which relates to the average BS power consumption and the average Tx power, is used. Total BS power consumption is composed of two components: the first is the Tx power dependent component expressed in the form of coefficient, which includes the PA and feeder losses with part of site cooling power consumption. The rest of the cooling power consumption, battery backup and signal processing power consumption is represented in the second part, which is constant and independent on Tx power. For modeling the power consumption of macro and micro Long Term Evolution (LTE) BSs, the authors in [11] have assumed a similar linear model with the distinction that Tx power dependent consumption is also expressed as a function of the traffic load. Based on the measurements performed on fully operated GSM

(Global System for Mobile Communications) and UMTS (Universal Mobile Telecommunications System) BS sites, we have also developed a precise linear power consumption model which relates average traffic load and average instantaneous power consumption [12].

The authors in [13] have assumed curves of nearly linear interdependence between different Tx power levels and the power consumptions of various BS components for different types of LTE BSs: macro, micro, pico and femto. It is shown that the total power consumption of macro BSs components are significantly Tx power dependent, while there is negligible Tx power dependency for pico and femto BSs. In fact, considerably lower Tx power in pico and femto BSs causes idle (fixed) power consumption to become dominant over the Tx dependent power consumption component. The power consumption model, in which Tx power dependent and idle power consumption components are qualified by the maximum Tx power of BS, is introduced in [14]. The authors concluded that although dense deployment of micro BS reduces Tx power, network energy efficiency is degraded because idle power consumption share becomes dominant in overall power consumption.

Partially opposing judgment is presented in [15]. It is shown that the deployment of femto BSs or any heterogeneous combination of BSs, instead of only macro BSs, results in reduced total Tx power in the analyzed area. Thus associated power consumption is also reduced. According to the algorithm proposed in [16], when traffic loads are low it is possible to reconfigure 3-sector macro BSs to omnidirectional BSs with appropriate Tx power. Since radio equipment that covers switched off sectors is in idle state, significant energy savings are achieved. Sleep modes with cell zooming as an energy saving technique based on the adaptation of a BS's Tx power are proposed in [17]. Also, in studies [18] and [19], we have proposed an energy-efficient management scheme based on dynamic access points (APs) or BSs on/off switching in combination with Tx power scaling, respectively. Significant energy savings on the level of complete network have been achieved.

In addition, energy savings can be obtained using an algorithm proposed in [17]. Installed on the control server, such an algorithm is especially suitable for implementation in networks with smaller cells. Based on load conditions and the distribution of mobile stations (MSs), the control server decides whether reference and neighboring BSs should adjust the transmission to assess energy savings through combining sleep mode and cell zooming techniques. Since BSs are limited by maximum Tx power they are also limited in the associated size of coverage area. This can be a disadvantage for some scenarios where cell zooming is applied. Under the assumptions that for such BSs low traffic load periods are dominant, the adequate solution for achieving better energy efficiency is the allocation of a higher number of BSs with smaller cells [20].

In [21] the authors analyzed cell wilting and blossoming techniques characterized with progressive decrease or increase of BS Tx power until the BS is switched off or on, respectively. The obtained results show that for the case of small cells, sleep and wake-up transients realized through linear reduction, and exponential increase of Tx power, are short and can be performed in maximally 30 s.

Cell sleeping can be used in combination with a coordinated multipoint (CoMP) technique. This technique enables BS Tx power reduction, but at the same time more power is consumed for signal processing. A combination of these techniques improves network energy efficiency since it ensures better Bit per Joule and spectral efficiency trade-off for high data rates [22]. The authors in [23] have shown that through multicell cooperation, significant energy savings can be achieved since techniques like joint transmission and cooperative beamforming improve signal quality and create space for Tx power reduction. For LTE networks, the energy-efficient self-organizing network (SON) architecture is based on intelligent cooperation between BSs, as proposed in [24]. Neighboring BSs interact with each other and, based on the network traffic, dynamically adjust Tx power levels and transition between on/off states.

According to the presented research activity, dynamic adaptation of BSs Tx power or on/off activity are commonly accepted as important assets of each approach, which consider energy-efficient management of cellular network resources. In order to have the correct estimations regarding savings that such approaches can offer, precise knowledge about how scaling Tx power or on/off BSs switching influences BS power consumption is of great importance. Also, in the literature all power consumption models used for analyses are based on assumptions instead of real measurements. They are simplified models characterized with linear interdependence among Tx and consumed BS power. To the best of our knowledge, this is the first paper to present precise models of Tx and consumed power interdependence for 2G, 3G and 4G macro BSs. Models are developed using principles of linear regression according to the obtained measurements performed on real BSs. By knowing exactly how the scaling of Tx power or on/off switching of BS components influence instantaneous

Table 1. GSM BS1 and GSM BS2 technical characteristics

Technical characteristics	GSM BS 1	GSM BS 2
BS location	BSS2	BSS2
Access technique	TDMA	TDMA
Year of base station model production	2000	2005
Weight (kg)	226	230
Temperature range (°C)	+5 do +40	+5 do +40
Dimensions (mm)	1900x600x400	1850x600x400
Frequency band (uplink)	880-915 MHz	880-915 MHz
Frequency band (downlink)	925-960 MHz	925-960 MHz
Sectors covered by BS	2 (C/B)	2 (A/B)
Number of TRUs per sector for voice carrier	3/1 (C/B)	2/2 active and 2 idle (A/B)
Number of TRUs per sector for data carrier	1/1 (C/B)	2/0 (A/B)
Number of PAs per sector	4/2 (C/B)	4/4(2 idle) (A/B)
Total number of PAs/BS rack	6	8 (2 idle)
Horizontal coverage area of BS	240°	240°
Number of antennas per sector	4/2 (C/B)	4/2 (A/B)
Number of CDUs in BS	3	3
Measured supply voltage	24 V DC	24 V DC
Maximal output Tx power	44.5 dBm	44.5 dBm

power consumption will enable precise estimation of energy savings. Hence, such models can be of huge importance to all future research efforts dedicated to the development of solutions for the energy-efficient management of radio resources in mobile operators' networks.

3. Overview of analyzed technologies

In order to relate instantaneous BS power consumption and Tx power, we have performed on-site measurements of five different, fully operated macro BSs. These BSs differ in transmission technology and production years. The first two are GSM, the next two are UMTS while the last one is a LTE BS. In the rest of the paper we will use notations GSM BS1 and GSM BS2 for GSM BSs. Similarly, UMTS BSs and LTE BS will be marked as UMTS BS1, UMTS BS2 and LTE BS1, respectively.

BSs on which measurements were performed are located at three different macro BS sites (BSSs). UMTS BS1 is placed at the first (BSS1), GSM BS1, BS2 and UMTS BS2 are allocated at the second (BSS2), while LTE BS1 is located at the third site (BSS3). These sites are among the most loaded sites and are placed in the urban area of a densely populated medium sized city.

BSs of the same technology (GSM BS1/BS2 or UMTS BS1/BS2) operate on the same frequency band, but they are manufactured in a different production years and belong to different product series (Tables 1 and 2). GSM BS1 is older than GSM BS2, while UMTS BS1 is older than UMTS BS2. On the other hand, LTE BS1 is the newest (Table 3).

According to BSs declarations, the nominal power supply voltage for UMTS, LTE and GSM BSs is also different. It is a 24 V direct current (DC) for GSM while for UMTS and LTE BSs equals to 48 V. However, on all analyzed BSSs, only 48 V DC BSs power supply systems with corresponding batteries are installed. Thus, to ensure required power supply voltage, internal DC/DC converters are used at the GSM BSSs. In Tables 1, 2 and 3, the exact voltage level of DC power supply system is noted the moment measurement of the electric current is performed. All analyzed BSSs are on-grid sites connected to AC (alternating-current) electrical network of 220 V and frequency 50 Hz.

In general, the components of each on-grid BSS can be classified according to their functions: radio equipment (BSs rack(s) with combiners, feeders, antennas), transmission equipment (microwave link and switches),

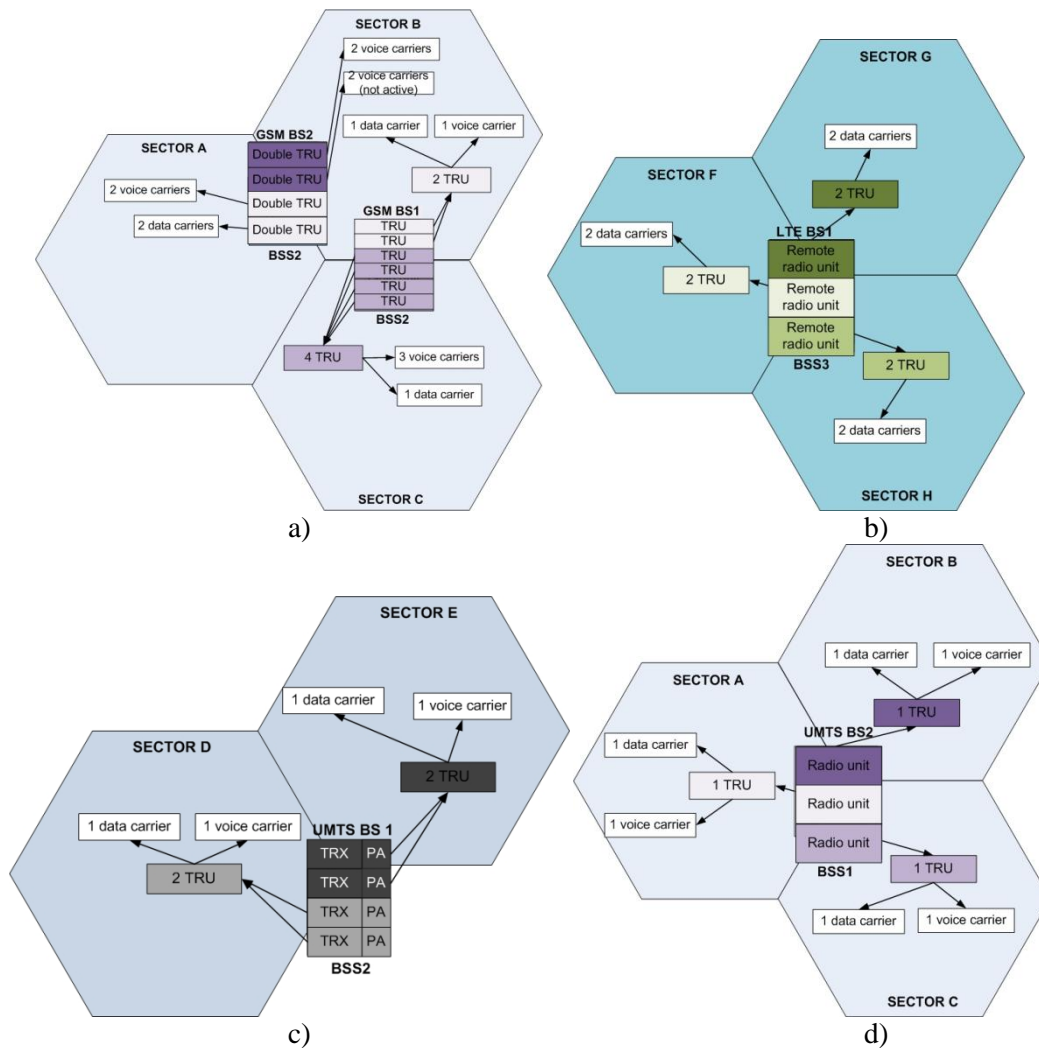


Figure 1. Configurations of analyzed BSs in terms of number of TRU/sector for: a) GSM BS1 and BS2 installed on BSS2, b) LTE BS1 installed on BSS3, c) UMTS BS1 installed on BSS1 and d) UMTS BS2 installed on BSS2

power supply system (battery, AC/DC or DC/DC converters) and the cooling equipment (air conditioner). Changes of the BS Tx power influence on almost all BSS components. Higher Tx power results in higher power consumption of BS and also in higher heat dissipation due to the warming of BS components, such as a PA. Higher heat dissipation requires higher energy for preserving equipment installed on BSS (batteries, BSs) in the temperature range prescribed for normal operation.

3.1. Description of GSM BS1 and BS2

According to Table 1, the main radio components of GSM BS1 are the transceiver unit (TRU) and the combining and distribution unit (CDU). The TRU contains three main parts: the transmitter with a PA, receiver, and digital signal processor. The TRU transmits and receives the radio frequency signals that are forwarded to and from the BS, respectively. Also, this unit processes signals at the air interface. The maximal number of TRU modules per one GSM BS cabinet is six (Table 1). Each TRU unit supports one radio carrier which serves up to eight full duplex or 16 half duplex time divided physical channels. In the case of voice communication between the BS and a mobile station (MS), four out of eight channels are used for transfer of signaling information. For data communication based on EDGE (Enhanced Data Rates for GSM Evolution) technology, six signaling channels are necessary. With the antenna system mounted on top of the building, TRUs communicate over CDU and contains a combiner, receiver/divider, amplifiers, and a duplexer. Hence, CDU represents an interface between TRU and antennas. Depending on the type, one CDU unit can handle a different number of TRUs.

Table 2. UMTS BS1 and UMTS BS2 technical characteristics

Technical characteristics	UMTS BS 1	UMTS BS 2
BS location	BSS1	BSS2
Access technique	WCDMA	WCDMA
Year of base station model production	2004	2010
Weight (kg)	210	230
Temperature range (°C)	+5 do +40	+5 do +40
Dimensions (mm)	1705 x 600 x 450	1485 x 600 x 483
Frequency band (uplink)	1920-1980 MHz	1920-1980 MHz
Frequency band (downlink)	2100-2170 MHz	2100-2170 MHz
Sectors covered by BS	2 (D/E)	3 (A/B/C)
Number of TRUs per sector for voice carrier	1/1 (D/E)	1/1/1 (A/B/C)
Number of TRUs per sector for data carrier	1/1 (D/E)	1/1/1 (A/B/C)
Number of PAs per sector	2/2 (D/E)	2/2/2 (A/B/C)
Total number of PAs/BS rack	4	6
Number of CDUs in BS	Part of antenna interface unit	integrated in radio unit
Horizontal coverage area of BS	240°	360°
Supply voltage	53.3 V DC	52.75 V DC
Maximal Tx power of pilot channel	33 dBm	33 dBm

The main technical improvement in hardware construction of newer GSM BS2 is visible in the implementation of TRUs. In fact, TRU modules are commonly replaced by double TRU (dTRU) modules. The dTRU contains two transceivers and has the same size as the TRU of GSM BS1. In comparison with GSM BS1, this means that capacity of the entire BS is doubled. However, other parameters such as size and weight (Table 1) of both GSM BSs of the same manufacturer are almost identical. Also, a novelty in GSM BS2 is that hybrid combiners are implemented as part of dTRUs. This is an important advantage since it enables application of the *smart range technique*. Classically, TRUs and antenna systems are connected in a way that each TRU is connected to its own antenna. Yet, sometimes it may be required to ensure greater capacity while the number of antennas is kept the same. In such a case, smart range configuration is suitable for practical application. By means of hybrid combiners the single dTRU (two TRUs) connects to the single antenna. However, the unwished consequence of such a configuration is that the Tx power is double reduced. Thus, to keep an appropriate level of coverage it is necessary for an additional number of classically connected TRUs over which primarily pilot signals will be transmitted.

On the BSS2 where we have performed measurements, GSM BS1 and GSM BS2 are configured in such a way that they cover three different sectors around BSS, with a radiation pattern of 120°/sector (Figure 1a). GSM BS2 covers sector A while GSM BS1 covers sector C. Sector B is covered using TRUs and other hardware elements from both GSM BSs racks (BS1 and BS2).

For transmission of voice carriers in sector C, three TRUs of GSM BS1 are used. In addition, one TRU module of EDGE technology is used for the data transmission by the carrier. Hence, to cover sector C four TRUs are used. Each of these contains one PA. Maximal output for GSM BSs is 44.5 dBm (28.18 W).

In sector A, two dTRUs (four TRU) are used for transmission (Figure 1a). One dTRU carries two voice carriers while the other dTRU handles two data carriers. Thus, for transmission in sector A, four PAs are used.

For covering sector B, two dTRU modules are used from GSM BS2 (Figure 1a). When the measurements were performed, one dTRU was in active state and the other was in standby (idle) state. Since each dTRU module contains two TRU modules, it also contains two PAs. Over each dTRU, two voice carriers are carried. With antenna elements they are connected over hybrid combiners using the smart range technique. This means that 4 TRUs are connected on two antennas, but the maximal output power of 44.5 dBm is reduced by half. Thus, to accomplish the required coverage level, voice pilot signals are transmitted over one TRU module of GSM BS1 (Figure 1a). Data signals are also carried over TRU of EDGE technology, which is part of GSM BS1. Figure 1a summarizes the TRU distribution among sectors and GSM BSs on analyzed BSS. In total, sector A and C are covered with 4 TRUs. On the other hand, sector B is covered in total with 6 TRUs, two of which are in idle state and two with half reduced output power. Each transceiver contains a corresponding PA.

Table 3. LTE BS technical characteristics

Characteristics of on-Site Base Stations	LTE BS
BS location	BSS3
Access technique	OFDMA
Year of base station model production	2012
Weight (kg)	9 (DU) 20 (RRU)
Temperature range (°C)	5 to +40 (DU) -40 to +55 (RRU)
Dimensions (mm)	66×482×350 (DU) 600×350×112 (RRU)
Frequency band	1800 MHz
Bandwidth	20 MHz
Number of BS racks	1
Sectors covered by BS rack	3 (F/G/H)
Number of TRXs per sector (data carrier only)	2/2/2 (integrated in RRUs)
Number of PAs per sector	2/2/2
Total number of PAs/BS rack	6
Number of antennas per sector	2/2/2
Horizontal coverage area of BS	360°
Number of combiners in BS rack	integrated in RRUs
Supply voltage	53.9 V DC
Maximal Tx power	40 W

3.2. Description of UMTS BS1 and BS2

Table 2 presents technical specifications of analyzed UMTS BSs. In the case of UMTS BS1, TRUs and PAs are separate components. The same PAs can amplify voice and data carriers. This type of PA is known as a multi-carrier power amplifier (MCPA). The TRUs handle digital/analog (D/A) and A/D conversion and modulation-demodulation of signals. The TRUs and PAs are connected to antenna through the antenna interface unit, which contains low noise amplifiers, radio frequency (RF) filters, combiners and splitters.

UMTS BS1 covers two sectors corresponding to 240 degrees of horizontal coverage around the BSS (Figure 1c). According to Figure 1c, each sector is covered by two TRUs. Voice traffic is carried over one of them and data traffic is carried over the second one. There are two MCPAs for each sector, configured in a way that one amplifies the voice carrier while the other amplifies the data carrier.

UMTS BS2 is a multi-standard BS which supports GSM, UMTS and LTE technology inside the same BS rack. In the current configuration, BS2 contains only UMTS modules. All radio equipment of this BS is implemented inside the unique module which contains PAs, transceivers, combiners and RF filters. According to Figure 1d, the UMTS BS2 rack covers three sectors around BSS. In order to cover each sector, one TRU, which is part of one radio unit (RU), is used. Each RU contains two MCPAs: one of them amplifies the voice carrier and the other one amplifies the data carrier.

3.3. Description of LTE BS1

The digital unit (DU) and remote radio unit (RRU) are the main parts of the analyzed LTE BS1 (technical characteristics can be found in Table 3). The RRUs, also known as remote radio heads, are outdoor elements mounted near the antennas. They are connected with the central DU located inside the BS rack through the bidirectional fiber optic link (Fiber-To-The-Antenna: FTTA). Such distributed BS architecture has become commonly accepted as one of the most important subsystems for BSs of later generations. The RRU contains

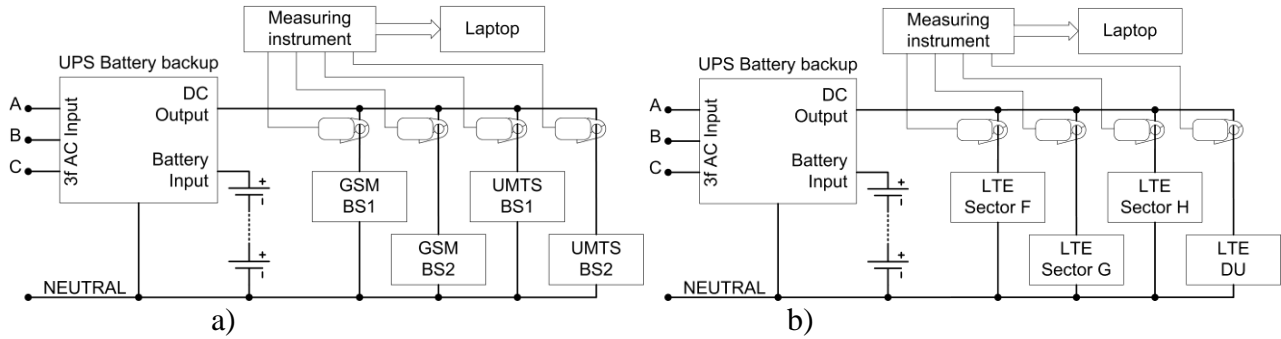


Figure: 2. Block diagram of measurement setup used for measuring instantaneous DC electric current draw of BSs installed on: a) BSS1 or BSS2 and b) BSS3.

Integrated RF front-end elements and functionalities, such as PAs, D/A and A/D converters, up/down converters, and operation and management processing capabilities. With this kind of configuration, significant energy savings are achieved since feeder losses are minimized. It is indicated in [25] that such a remote radio system reduces BS network energy consumption by 25 to 50 percent, depending on the system configuration, and also contributes to a minimization of BS rack dimensions (Table 3). However, such a configuration in most cases demands a separate power supply for each RRU and DU.

The DU provides the full internet protocol (IP) connectivity of the LTE BS1. Among other functions, it also ensures control, baseband, switching and traffic management interfaces. The DU of the LTE BS1 is currently configured to support only LTE data traffic and the power consumption of DU is independent on the Tx power. Inside the analyzed LTE BS1 rack, one DU with a fixed power consumption of 61.98 W is installed. In the case of the analyzed LTE BS1, this DU manages activity of three RRUs. According to Figure 1b, the LTE BS1 rack (DU) covers three different sectors around BSS3. For radio coverage of each sector two TRXs are used, each containing its own PA. These TRXs constitute the main part of RRUs, and in the case of analyzed BSS3 one RRU per sector is connected with the antenna system and is used for covering the corresponding sector.

4. Measurements and modeling approach

4.1. Measuring setup

The instantaneous power consumption of BS is defined as a product of the instantaneous DC electric current and the associated DC power supply voltage. The measured voltage of the DC battery power supply is constant in time, and for individual GSM, UMTS and LTE BSs is listed in Tables 1, 2 and 3, respectively. According to the block diagrams presented in Figure 2a) and b), we perform continuous measurements of the electric current drawn for the case of BSs installed on the BSS1/BSS2 and BSS3, respectively. Measurement schemes applied on BSS1/BSS2 and BSS3 differ due to the fact that LTE RRUs and DU have separate power supplies which must be separately measured. Measurements were performed during changes of the Tx power levels, which are recorded from the BSs software configuration interface. The electric current drawn for each BS is measured using the following equipment: a multi-channel measuring instrument Handyscope HS4, a laptop with specialized measuring software installed, current clamps, and associated cables.

Handyscope HS4 (TiePie Engineering) is a multi-channel measuring instrument that integrates four different measuring capabilities: oscilloscope, spectrum analyzer, multimeter and data logger. It has the capability of concurrently detecting up to four input measuring signals. In our case, measured signal is the DC current flowing through the power supply cable of each BS rack.

For precise detection of lower currents we use Fluke i30s, while for detection of currents of higher values (above 20 A) we use Chauvin Arnoux PAC 22 current clamps. Current clamps were connected on input channels of the multi-channel measuring instrument (Figure 2). The measured signals are concurrently transferred to the laptop through a USB connection. They are displayed in multi-channel software that is specially designed to work with the Handyscope HS4 instrument.

The frequency of samples used for capturing the DC consumption was set up to 5 kHz on each of the measuring channels. The samples were filtered using a low-pass filter of 0.1 Hz and finally re-sampled to 1 Hz. This

resulted in 1 measuring sample taken every second. It is reasonable to believe that such an approach guarantees acceptable measurement accuracy.

All measurements were performed on fully operated BSs during peak hours. Since continuous measurements were performed during relatively short time period, influence of users voice or data traffic is neglected. We refer the reader to [12] for the explanations on how traffic variations influence on daily instantaneous power consumption of BSs.

4.2. Linear modeling

In order to develop models that relate the instantaneous power consumption of BSs to current Tx power, we used an approach based on linear mathematical modeling. By knowing the average instantaneous power consumption for each Tx power level, our goal was to develop precise linear power consumption models for every analyzed BS, which differs in access technology and oldness. The developed models must express instantaneous power consumption of each BS rack as a function of the current Tx power. In order to model the interdependence between the power consumption of each BS rack and corresponding Tx power, we used the following equation:

$$y = \beta_1 f_1(x) + \beta_2 f_2(x) + \dots + \beta_p f_p(x) = F(x, \boldsymbol{\beta}) \quad (1)$$

According to the relation (1), response y is modeled as a linear combination of functions of independent variable x . In expression (1), $f_j(x)$ ($j = 1, \dots, p$) are the *terms* of the model, while β_j ($j = 1, \dots, p$) represents the *coefficients*. Up to p different terms and corresponding coefficients are assumed.

For n independent observations $(x_1, y_1), (x_2, y_2), \dots, (x_n, y_n)$, expression (1) can be written in the matrix shape:

$$\begin{bmatrix} y_1 \\ y_2 \\ \vdots \\ y_n \end{bmatrix} = \begin{bmatrix} f_1(x_1) & f_2(x_1) & \dots & f_p(x_1) \\ f_1(x_2) & f_2(x_2) & \dots & f_p(x_2) \\ \vdots & \vdots & \ddots & \vdots \\ f_1(x_n) & f_2(x_n) & \dots & f_p(x_n) \end{bmatrix} \begin{bmatrix} \beta_1 \\ \beta_2 \\ \vdots \\ \beta_n \end{bmatrix} \quad (2)$$

or, in a short matrix notation:

$$\mathbf{y} = \mathbf{f}\boldsymbol{\beta} \quad (3)$$

where the \mathbf{f} in relation (3) is the design matrix of the system (Jacobian). In general, Jacobian can be calculated as:

$$f_{ij} = \frac{\partial F(x_i, \boldsymbol{\beta})}{\partial \beta_j} \quad (4)$$

and solution of the matrix equation (3) is:

$$\boldsymbol{\beta} = (\mathbf{f}^T \mathbf{f})^{-1} \mathbf{f}^T \mathbf{y} \quad (5)$$

In our case, we approximate the function of the model through a linear regression model with only two unknown coefficients: β_1 and β_2 . All other parts can be replaced by a random error ε and relation (1) can be written as:

$$y_i = \beta_1 + \beta_2 x_i + \varepsilon_i \quad (6)$$

where the linear regression model becomes an $n \times 2$ system of equations.

Uncontrolled factors and experimental errors are modeled in relation (6) by error ε , and assumed to be uncorrelated and distributed with zero mean and constant variance. To fit the model with the data, the system must be solved for the coefficients β_1 and β_2 . The error can be calculated as the difference between the measured output and the modeled output expressed as:

$$\boldsymbol{\varepsilon} = \mathbf{y} - \mathbf{f}\boldsymbol{\beta} \quad (7)$$

and the goal is to minimize the sum of squares of these errors according to the next expression:

$$M = \sum_{k=1}^p (\varepsilon_k)^2 = \boldsymbol{\varepsilon}' \boldsymbol{\varepsilon} = \min \Rightarrow \frac{\partial M}{\partial \boldsymbol{\beta}} = \frac{dM}{d\boldsymbol{\varepsilon}} \frac{d\boldsymbol{\varepsilon}}{d\boldsymbol{\beta}} = -2\boldsymbol{\varepsilon}' \mathbf{f} = \mathbf{0} \quad (8)$$

Finally, using rule for transposition, like in equation (5), we have a solution for coefficients expressed as:

$$\mathbf{f}' \boldsymbol{\varepsilon} = \mathbf{f}' (\mathbf{y} - \mathbf{f}\boldsymbol{\beta}) = 0 \Rightarrow \boldsymbol{\beta} = (\mathbf{f}' \mathbf{f})^{-1} \mathbf{f}' \mathbf{y} \quad (9)$$

For calculation of a confidence interval, we need a variance s of coefficients β_1 and β_2 . The approximate variance-covariance matrix of the regression coefficients is estimated by [26]:

$$\mathbf{s}^2(\boldsymbol{\beta}) = \frac{\boldsymbol{\varepsilon}' \boldsymbol{\varepsilon}}{n - p} (\mathbf{f}' \mathbf{f})^{-1} \quad (10)$$

Residual mean square has $n - p$ degrees of freedom associated with it, since p parameters need to be estimated in the regression function of our model.

In our linear model the terms of Jacobian are $f_1(x) = 1$ and $f_2(x) = x$. The estimated standard uncertainty of coefficient β_1 expressed in watts of consumed power (W) is on $s(1,1)$ of \mathbf{s} matrix. On the other hand, β_2 is on $s(2,2)$ element of matrix \mathbf{s} . For a normal distribution, standard uncertainty covers the confidence level of approximately 68 percent. Multiplying the standard uncertainty by a coverage factor k provides the result, which is called the expanded uncertainty. Most commonly, uncertainty is scaled by using the coverage factor $k=2$ in order to give a level of confidence of approximately 95 percent [27]. This level of confidence is also used in our analyses.

5. Results of measurements

5.1. Tx power adaptation of GSM base stations

In total, we have performed per each GSM BS rack two different measurements of interdependence between instantaneous BSs power consumption and Tx power. In each measurement, approximately every two minutes Tx power was scaled from 47 dBm to 35 dBm in steps of 2 dBm. Hence, measurement results are obtained for 7 different Tx power levels. Additionally, measurement results were recorded for the case of putting TRUs in standby mode through complete deactivation or reactivation of TRUs.

Measurements are firstly performed on GSM BS1. In the first measurement, only four TRUs that cover sector C are in the active state (Figure 1a), while the other two TRUs used for covering sector B are shut down (in standby mode). In the second measurement all six TRUs inside the BS rack are active. Similar measurements were performed on GSM BS2. During the first measurement only, TRUs that cover sector A are active, while TRUs used for covering sector B are turned off. During the second measurement, two TRUs that cover sector B are also in active state. It is worth indicating that during all these measurements, on each Tx power level users traffic was transported over each TRU which was in active state.

5.2. Measurement results for GSM BS1 and BS2

Measurement results obtained for GSM BS1 and BS2 are presented in Figures 3a, 4a and Figures 5a, 6a, respectively. Figures 3a and 5a indicate influence of power consumption on Tx power for the case of complete GSM BS1 and BS2 racks, respectively. Furthermore, Figures 4a and 6a present the same interdependence for BS1 and BS2, respectively, in the case when only those TRUs used for covering one sector remain active. The vertical lines on each figure indicate time periods in which Tx power levels of GSM BSs are constant. In addition, in all figures the most right vertical lines indicate measuring periods during which TRUs inside associated BSs are turned off.

As expected, instantaneous power consumption decreases with a reduction of Tx powers during each of the performed measurements. This reduction of power consumption is clearly visible even for the lowest Tx power

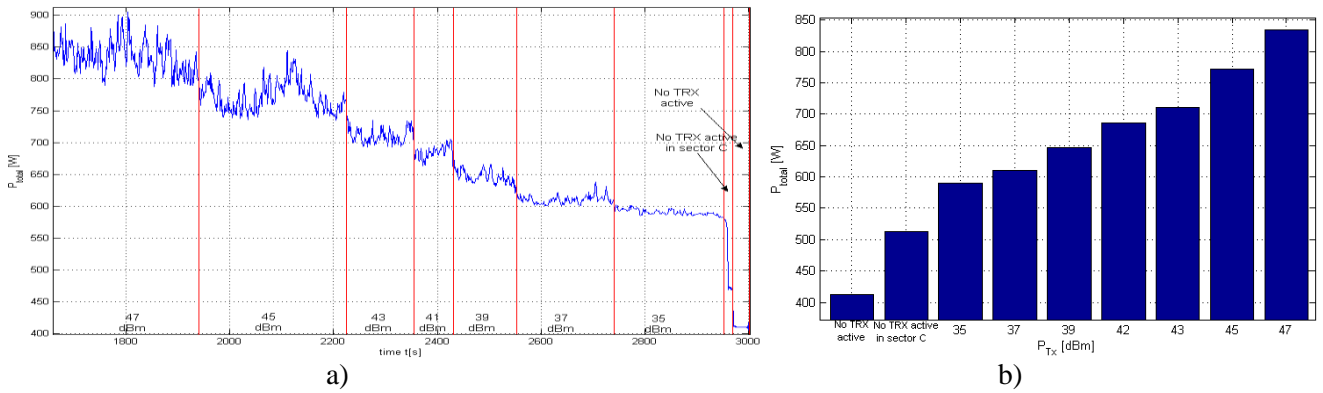


Figure 3. a) Measured and b) averaged interdependence among instantaneous power consumption and Tx power when all TRXs inside the GSM BS1 rack are active.

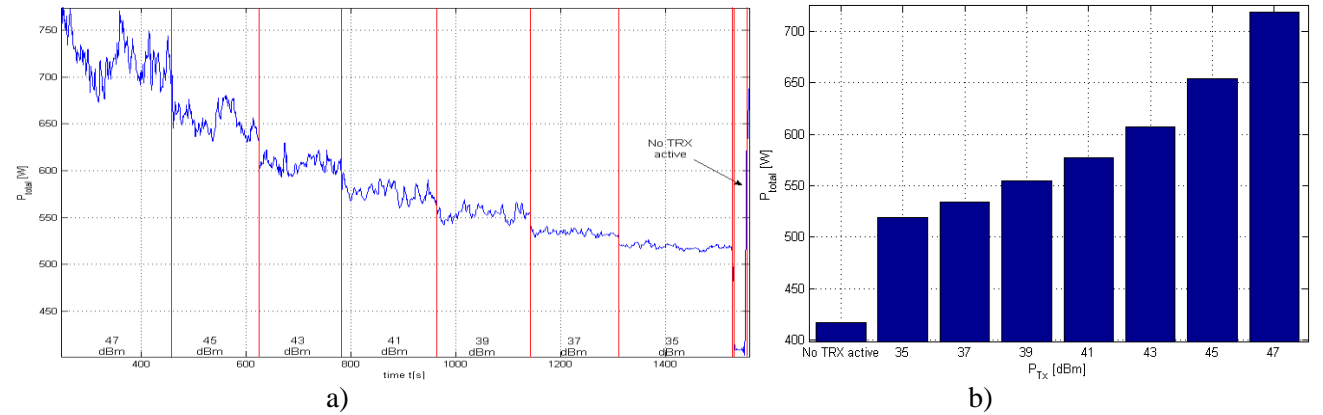


Figure 4. a) Measured and b) averaged interdependence among GSM BS1 instantaneous power consumption and Tx power when TRXs that cover sector C are active.

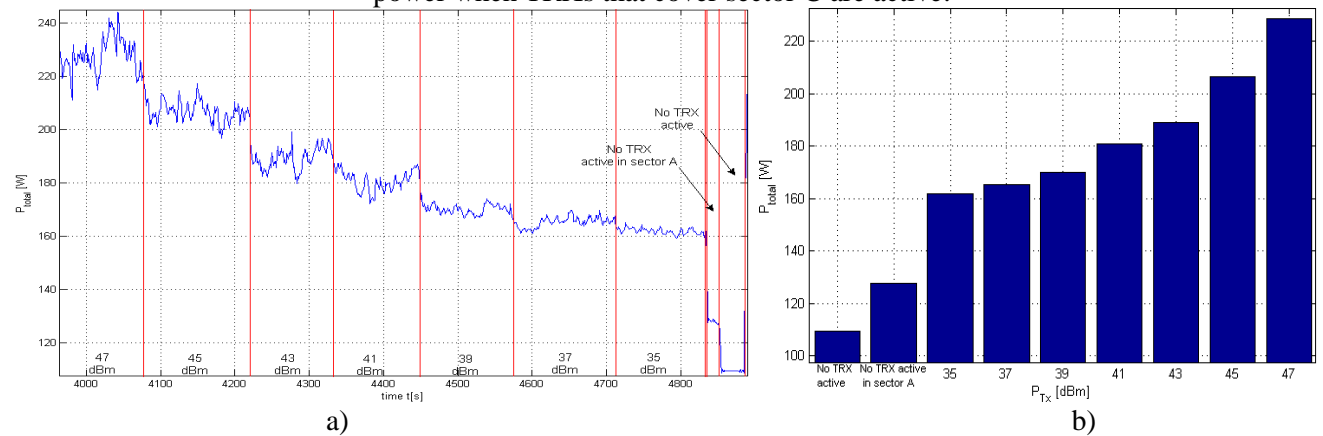


Figure 5. a) Measured and b) averaged interdependence among instantaneous power consumption and Tx power when all TRXs inside the GSM BS2 rack are active.

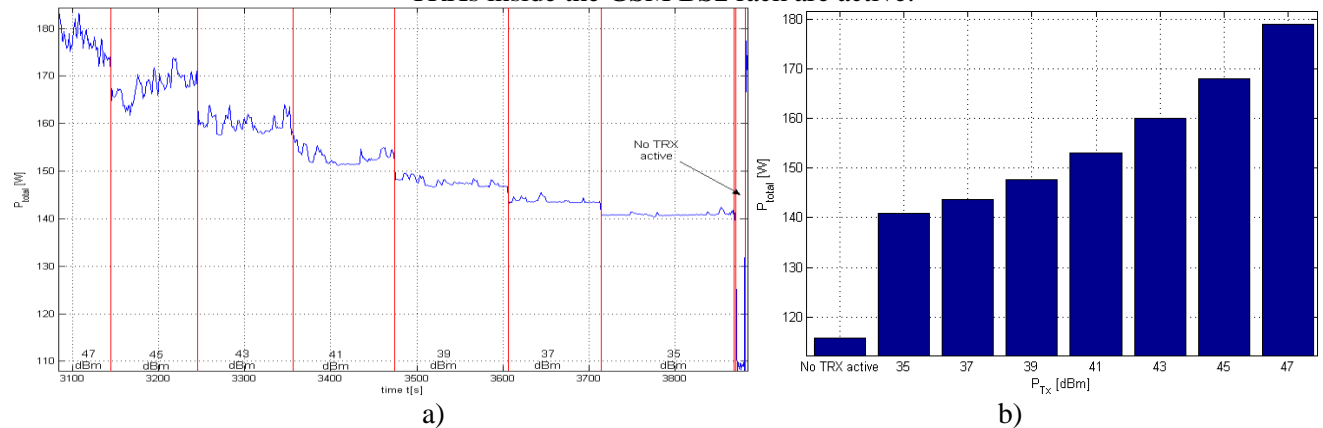


Figure 6. a) Measured and b) averaged interdependence among GSM BS2 instantaneous power consumption and Tx power when TRXs that cover sector A are active.

levels (change from 37 dBm to 35 dBm).

For the same levels of Tx power, instantaneous power consumption of the GSM BS2 is significantly lower when compared with those of GSM BS1 (Figures 3 and 5). The reason can be found in the hardware configuration of each BS and advances in development of hardware components. Although at the moment of measurements both BSs had an equal number of active TRUs (6 in the case of BS1 and 2x3dTRU in the case of BS2). The dTRUs of the newer BS2 consumes almost twice less power while ensuring equal capacity as described in Section 3.1.

The calculated average instantaneous power consumption of GSM BS1 and BS2 are presented for each level of the Tx power in Figures 3b, 4b and 5b, 6b, respectively. Similar power reduction profiles can be noticed on all figures. The changes in power consumption are the most significant for the highest Tx power levels. For example, the highest reduction of BS power consumption can be noticed for the first two intervals in which Tx power was reduced from 47 dBm to 45 dBm, and from 45 dBm to 43 dBm. This is due to logarithmic scaling of the Tx power.

It can be noted from Figures 3-6 that turning off all TRUs in GSM BS racks results in an approximate twofold reduction of instantaneous power consumption, when compared to those when all TRUs are active and transmit at the highest Tx power levels. Therefore, even when all TRXs are in standby state (turned off) GSM BSs still consume some power. This power is known as static or a fixed component of macro GSM BSs power consumption. It is a Tx power independent component and approximately equals half of the total BS consumption in the case of transmission at maximum Tx power. Another variable part of total BS power consumption is a Tx power dependent component and can contribute up to 50 percent of total BS power consumption.

In addition, from Figures 3 and 5 it can be noticed that shutting down all TRUs used for covering one sector can influence a reduction in the total instantaneous power consumption of a complete BS. This reduction will depend on the number of TRUs used per sector. In the case of shutting down sectors with a higher number of TRUs, a reduction of BS Tx power will be higher and vice versa. For example, from Figures 3b and 4b can be noticed that higher energy savings can be obtained in cases of shutting down BS1 TRUs used to cover sector C. This is because sector C has a higher number of TRXs and more energy is consumed to cover the sector when compared to sector B, for example. Nevertheless, even when the TRUs of one sector are all turned off, Figures 4 and 6 show that decreasing the Tx power in other active sectors will result in a decrease of the total instantaneous power consumption.

5.3. Tx power adaptation of UMTS base stations

In the case of macro UMTS BSs, generally it is not allowed through the BS configuration software to adapt the total Tx power level. Instead, the Common Pilot CHannel (CPICH) power level P_{Tp} was adjusted during the performed measurements. Hence, these measurements relate the BSs instantaneous power consumption and the CPICH Tx power level. It is worth indicating that, in practice, approximately 10 percent of the total Tx power belongs to the Tx power of the CPICH channel. On both of the analyzed UMTS BSs, a range of CPICH Tx power levels were adjusted between 31 dBm and 15 dBm. Between these two border levels the Tx power is changed in 1 dBm steps during each time interval lasting approximately 2 minutes. This results in 17 different Tx power levels. Analogously to GSM BSs, the periods in which TRX are completely deactivated or reactivated are also encompassed within the measurements.

Two different measurements were performed on the UMTS BS1. During the first measurement, all TRXs inside the BS cabinet cover two sectors (D and E) and are in the active state (Figure 1c). In the second, the measurements identify that the TRXs covering sector E are active and the TRXs that cover sector D are in standby (turned off) state. Additionally, we performed one measurement for the case when all TRXs inside the UMTS BS2 cabinet are active, and in all sectors they transmitted at equal CPICH Tx power level (Figure 1d). We did not perform a shutdown of some UMTS BS2 TRXs, since this BS with equal configuration covers all three sectors around BSS1, what enables estimation of consumed power for each sector. As in the case of measurements performed on the GSM BSs, users' traffic is transferred over the active TRXs in case of transmission at each of the scaled CPICH Tx power levels.

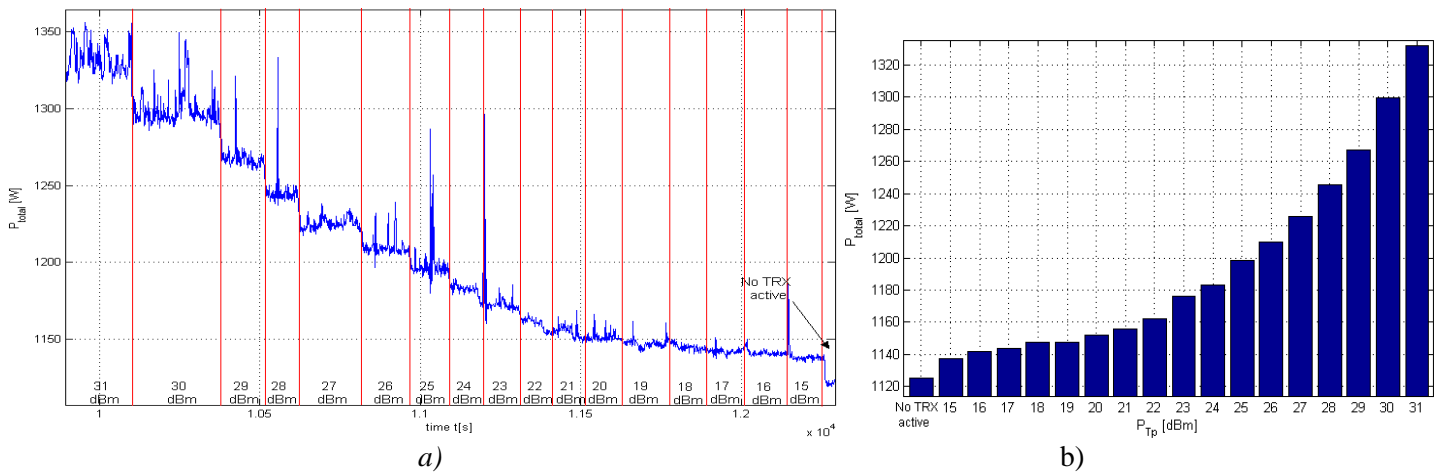


Figure 7. a) Measured and b) averaged interdependence among instantaneous power consumption and CPICH Tx power when all TRXs inside the UMTS BS1 rack are active.

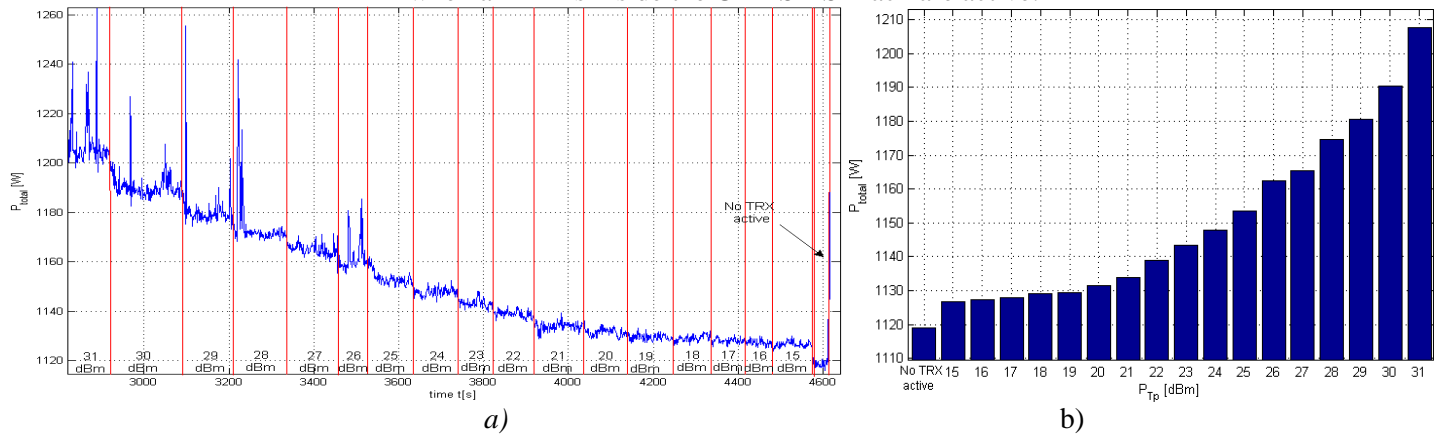


Figure 8. a) Measured and b) averaged interdependence among UMTS BS1 instantaneous power consumption and CPICH Tx power when only TRXs that cover sector E are active.

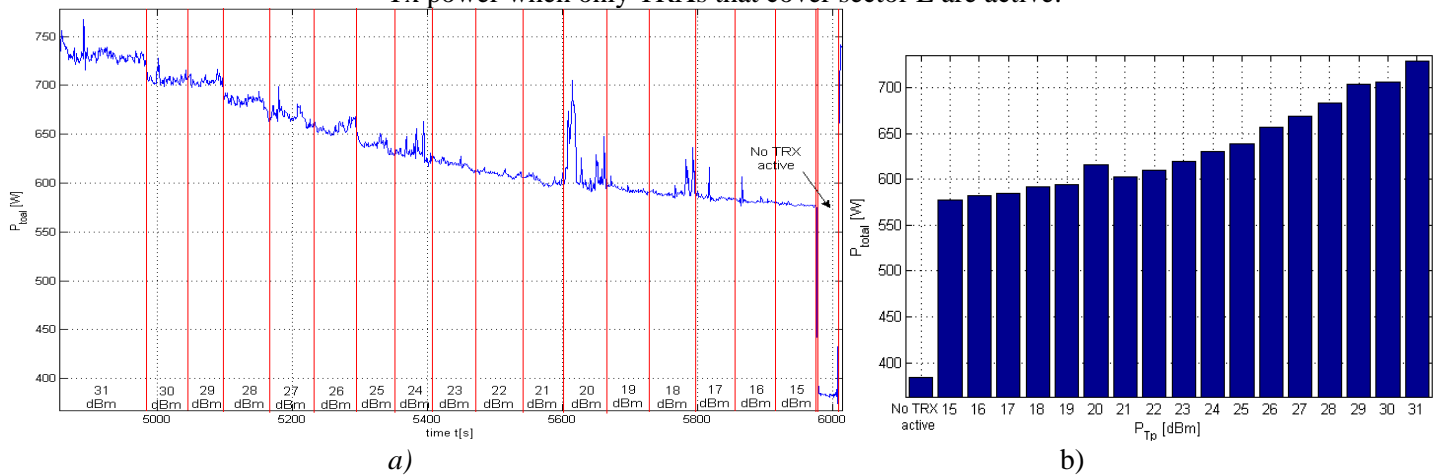


Figure 9. a) Measured and b) averaged interdependence among instantaneous power consumption and CPICH Tx power when all TRXs inside the UMTS BS2 rack are active.

5.4. Measurement results for UMTS BS1 and BS2

Figures 7a, 8a and 9a present measurement results obtained for the UMTS BS1 and UMTS BS2, respectively. Analogously to the presentation of measuring results for the GSM BSs, measuring periods during which Tx powers have constant values or TRXs are in idle state are marked with vertical lines in each figure. Figures 7a and 9a show interdependence of consumed and CPICH Tx power for complete UMTS BS1 and BS2 racks, respectively. In addition, the graph on Figure 8a depicts the measurement results for the case when the TRXs dedicated to cover sector E of BS1 are in standby state (turned off).

The average values of instantaneous UMTS BSs power consumption are presented for each CPICH Tx power in Figures 7b, 8b and 9b. As in the case of GSM BSs, measuring the results presented in Figures 7a, 8a and 9a indicate that a decrease of the CPICH Tx powers is followed with a decrease in the instantaneous power consumptions of the UMTS BSs. Similarities with the results obtained for GSM BSs can be found in the fact that variations in UMTS BSs power consumption are again the most significant for a few of the highest CPICH Tx power levels. It can be noticed that a significant reduction of the variable component of BS power consumption can be achieved by decreasing the Tx power by 3 dBm. For example, decreasing the CPICH Tx power from the highest level (31 dBm) to 28 dBm, results in a 45 percent lower variable component of BS power consumption.

In addition, the least steepest graph presenting the measurement results on UMTS BSs can be noticed when compared with those obtained for GSM BSs. This is due to the twice smaller gradient of the Tx power change, which is equal to 1 dBm of the CPICH Tx power. Hence, decreasing the Tx power using larger gradients will result in a larger decrease of the GSM and UMTS BSs instantaneous power consumption and vice versa.

From Figures 7b and 9b it can be seen that on equal CPICH Tx power levels, UMTS BS1 consumes more than BS2, even though the BS2 has a stronger configuration consisting of a higher number of TRXs (6) used for covering a higher number of sectors (Figures 1c and 1d). This is because UMTS BS2 belongs to the newest generation of UMTS BSs recently introduced to the market. Thus, all hardware components integrated inside the BS2 rack are newer and generally more energy-efficient than those of the UMTS BS1. This is especially true for RF PAs which have the highest influence on BSs power consumption. Due to advances in the efficiency of PAs, the newer UMTS BS2 has PAs with better efficiency. In comparison with UMTS BS1, this ensures lower power losses at equal CPICH Tx power levels.

UMTS BS1 and UMTS BS2 static power consumptions are presented in Figures 7b, 8b and 9b. In this figures, static power consumption is depicted as power consumption in periods in which all TRXs are in standby state. It can be noticed that the static share in the total power consumption of the UMTS BS2 is significantly lower than those of the UMTS BS1. Such disproportion is caused by fairly compact TRX modules of newer UMTS BS2, which integrate few different functional components inside a single module. Thus, by shutting down all TRXs of BS2, a larger amount of components that contribute to the reduction of the static part of BS power consumption are turned off.

Measured variations of instantaneous power consumption on specific Tx power levels can be noticed in Figures 3-6 for GSM BSs, and in Figures 7-9 for UMTS BSs. Visible oscillations are caused by variations in users traffic transferred over BSs transmitting at specific Tx power levels. In the paper [12], it is shown that instantaneous power consumption of BS somewhat increases when the amount of user traffic transferred over BS increases. Additionally, scaling Tx power imposes disconnections and associations of users what influence on the current number of users served by the BS. For that reason, the smallest variations of power consumption can be noticed on the lowest BS Tx power levels, since the lowest number of users can be connected and almost negligible traffic can be transported over macro BS.

During the measurements on UMTS BSs we have also noted the changes in power consumption caused by activation and deactivation of TRXs. These changes are depicted in Figure 10a and 10b for the activation and deactivation of all TRXs inside the UMTS BS1 and BS2 rack, respectively. Also Figures 10 presents results for activation and deactivation of TRXs used in some sectors. As expected, the highest decrease in power consumption is caused by deactivating all TRXs of the BS rack. The changes are less evident when two out of the four TRXs used to cover sector E of UMTS BS1 are deactivated. In this case, the smallest power consumption reduction is achieved in the moment when one out of two remaining active TRXs is deactivated.

Hence, the obtained measuring results show that the greater number of active TRXs inside the BS rack implies higher energy consumption. Thus, to achieve energy efficiency it is important that the number of active transceivers inside the BS rack is just enough to ensure required user capacity. For that reason, it is advisable to apply some of the solutions for dynamic TRXs activity control. Such solutions can ensure that a given number of TRXs can be deactivated during low load periods or activated when additional BS capacity resources are needed.

5.5. Tx power adaptation of the LTE base station

In the case of measurements performed on LTE BS1, the Tx power is decreased from maximal level of 40 W to

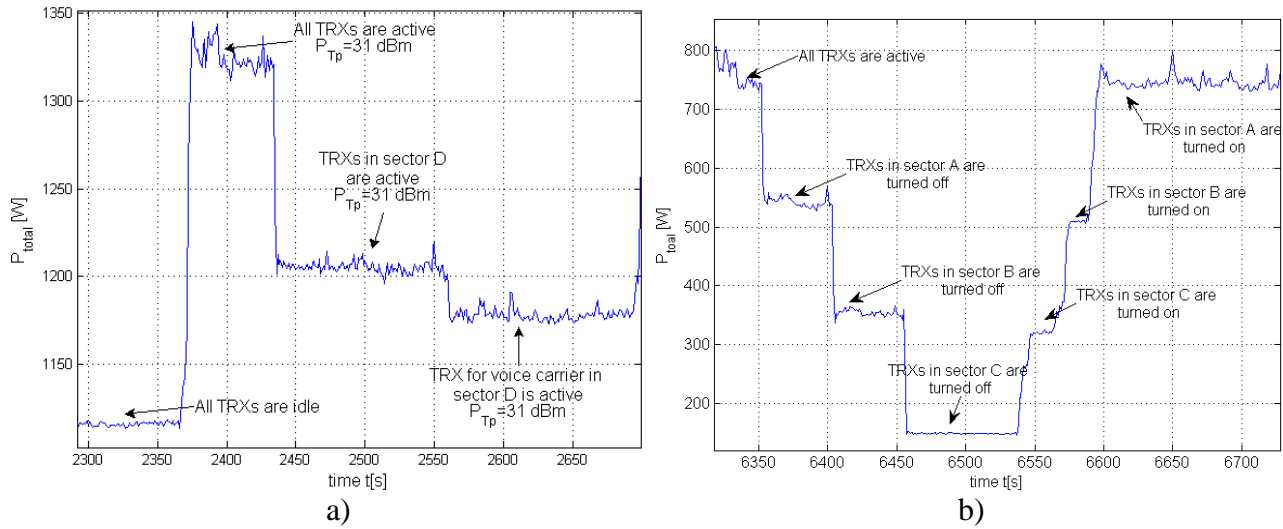


Figure 10. Changes of power consumption caused by TRX activations/deactivations for: a) UMTS BS1 and b) UMTS BS2.

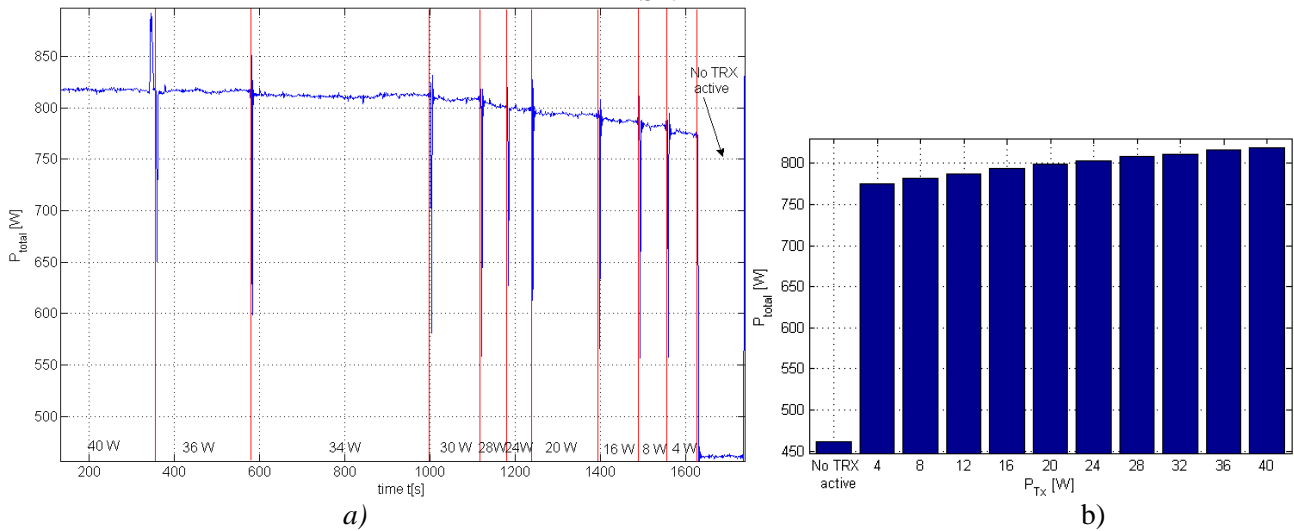


Figure 11. a) Measured and b) averaged interdependence among instantaneous power consumption and Tx power when all TRXs of LTE BS1 are active.

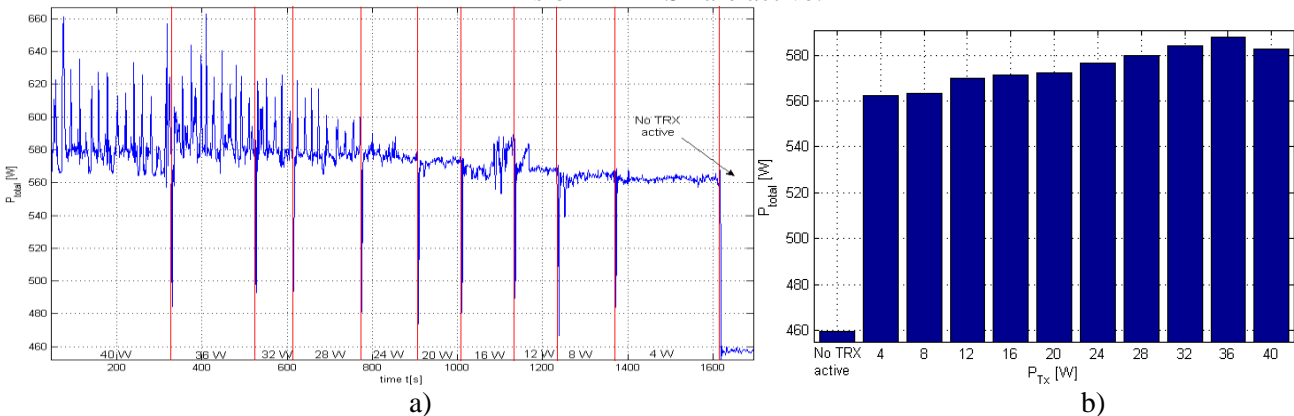


Figure 12. a) Measured and b) averaged interdependence among instantaneous power consumption and Tx power when TRXs that cover sector H of LTE BS1 are active.

the lowest levels. The Tx power is decreased in 10 percent decrements of maximal Tx power value (90%, 80%,...). Besides measurements performed for 10 time periods characterized with P_{Tx} corresponding Tx power levels, the measurement results were recorded for the case when some RRUs were completely turned off or on. Generally, LTE BSs have recently been implemented to offer an LTE service in the city area where measurements are performed. In a whole city area only a few macro LTE BSs were installed. Client devices like

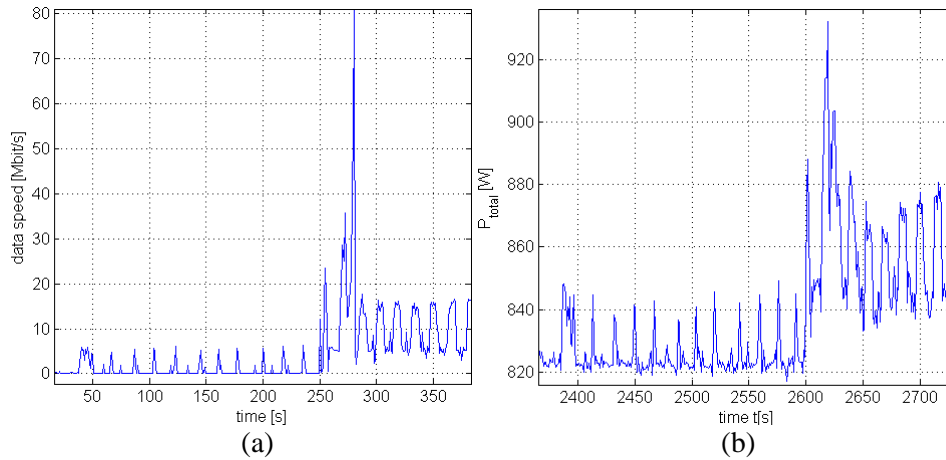


Figure 13. Presentation of measured results obtained during the same time periods for: a) instantaneous data rates and b) instantaneous LTE BS1 power consumption.

smart phones and USB modems which support LTE also appeared recently on the market. Thus the number of LTE users in a whole city is negligible, which means that the offered LTE BSs capacity is currently mostly unused.

Knowing this fact, we have performed two different measurements on LTE BS1 which cover three sectors (F, G and H) around BSS3 (Figure 1b). In the first measurement, we measured the power consumption of the whole LTE BS1 when there is no traffic load in the cells of each sector. In order to obtain more realistic results, during the second measurement we generated continuous data streaming by means of a laptop connected with BS through a LTE USB stick. In this measurement, a user with a LTE capable device was located in sector E and only the RRU covering this sector was active. The RRUs covering the remaining two sectors (F and G) was in standby state (turned off).

5.6. Measurement results for LTE BS1

The results of both measurements performed on the LTE BS1 are presented in Figures 11 and 12. Figure 11 presents results obtained when all TRXs of RRUs are active, while Figure 12 shows the results obtained when the TRXs of only one RRU, used to cover sector H, is active. Obtained measurement results are in line with previously presented results for the GSM and UMTS BSs, showing a decrease of the LTE BS1 power consumption when Tx power decreases. However, in comparison with the obtained results for GSM and UMTS BSs, these decreases are significantly smaller.

Two reasons cause such measured results. The first reason can be found in the newest hardware of the LTE BS1. Generally, latest generations of the LTE BSs are characterized with the PAs having significantly better efficiency than those implemented in older generations of the GSM and UMTS BSs. For that reason, the RF power dissipation is reduced and in comparison with the PAs of older BSs, lower input power is needed to ensure an equal level of output power. The second reason is related to the distributed BS architecture characterized with the removal of RUs from the BSs racks and its placement near the antenna elements. It is known that in the centralized BS architecture typical for GSM and UMTS BSs, about half of the output power from the PA is lost in the feeders [28]. Hence, to obtain the same level of radiated RF power in the antennas of a distributed BS system, a lower level of power is needed at the output of the PA in centralized BS architectures. These two reasons explain a small share of the variable component in the total BSs power consumption.

On the other hand, the DU has also a small share equal to 7.5 percent of the total BS power consumption and this consumption is constant over time. In the case of BSs with such a configuration (3 RRU and 2 TRX/RRU), the rest of the power consumption of approximately 90 percent is the power consumption of RRUs. Hence, 30 percent of the total power consumption goes to powering the RRU of each sector. Of this power consumption, 50 percent is static (stand by) power consumed even when the TRXs of the RRUs are in a turned off state. For that reason, from Figures 11b and 12b it can be noticed that approximately 50 percent of the total BS power consumption is static (stand by) and remains constant even when all TRXs in each RRU have been turned off.

From Figure 12a it can be noticed that traffic load generated by user activity influences an increase in BS power

Table 4. Calculated regression coefficients with linear models for analyzed BS types

BS type	$\beta_1 \pm 2s(1,1)$ [W]	$\beta_2 \pm 2s(2,2)$	Power consumption model
GSM BS1	598.935±29.745	5.041±1.219	$P_{total}=5.041 * P_{tx}+598.935$
GSM BS1(sector C active)	517.201±12.692	4.165±0.52	$P_{total}=4.165 * P_{tx}+517.201$
GSM BS2	159.511±3.66	1.424±0.15	$P_{total}=1.424 * P_{tx}+159.511$
GSM BS2(sector A active)	141.107±3.593	0.802±0.147	$P_{total}=0.802 * P_{tx}+141.107$
UMTS BS1	1138.871±3.859	160.804±7.679	$P_{total}=160.804 * P_{tp}+1138.871$
UMTS BS1(sector E active)	1127.567±2.897	67.118±5.764	$P_{total}=67.118 * P_{tp}+1127.567$
UMTS BS2	588.705±8.827	128.68±17.567	$P_{total}=128.68 * P_{tp}+588.705$
LTE BS1	772.907±2.604	1.214±0.105	$P_{total}=1.214 * P_{tx}+772.907$
LTE BS1 (sector H active)	559.578±3.923	0.702±0.158	$P_{total}=0.702 * P_{tx}+559.578$

consumption at each Tx power level. More precisely, Figure 12b depicts average power consumptions of BS when only the TRXs of an RRU covering one sector are active. This RRU transfers data traffic generated from only one LTE user. It can be noticed in Figure 12b that BS power consumption at Tx power levels of 36W and 32W is higher than consumption at Tx power of 40W. This is because a user in this time period generates more traffic and utilizes more BS capacity than in the previous period.

To prove this, we present in Figures 13a and 13b an almost perfect correlation between instantaneous changes of traffic load and BS power consumption, respectively. Figure 13a presents a snapshot obtained from the software installed on the laptop with capability of monitoring and graphical visualization of instantaneous data rates. Figure 13b presents the changes in the power consumption of the entire BS in that time period. It is clearly visible that variations of the BS power consumption are precisely followed by variations of data rates. The reason for such behavior can be found in the access method, which for LTE BSs is based on orthogonal frequency division multiple access (OFDMA) technology. In the moment when a user starts transmission, a number of OFDMA subcarriers become scheduled for that user's data transmission. Subcarriers allocation and the signal processing required for this data transmission impose additional energy consumption, the variation of which closely follows such subcarrier allocations and processing.

6. Power consumption models

6.1. Models based on measured results

Based on the average instantaneous DC power consumption obtained for every Tx power level through measurements on each BS rack, we developed linear BSs power consumption models. The developed models express instantaneous power consumption of each BS rack as a function of the current Tx power. These models are developed by means of linear mathematical regression presented in Section 4.2. Calculation of the models is performed using function *regress* which is part of a Matlab software package.

Obtained linear power models for each measurement are shown in Table 4 and in Figures 14-16. The developed models are based on the next linear relations:

$$P_{total} = \beta_2 * P_{Tx} + \beta_1 \quad [W] \quad (11)$$

$$P_{total} = \beta_2 * P_{Tp} + \beta_1 \quad [W] \quad (12)$$

where values of the coefficients β_1 and β_2 for the BS racks of different technologies have been calculated and presented in Table 4. Both relations are derived from relation (6) where x_i in relation (11) corresponds to the total Tx power P_{Tx} (W) and in relation (12) to the (pilot) CPICH Tx power P_{Tp} (W). Relation (11) is used for modeling power consumption of the GSM and LTE BSs, while relation (12) models power consumption of the UMTS BSs.

The developed linear models have been plotted together with the measured results and the linear regression lines having 95 percent confidence region in Figures 14-16. These figures confirm that we managed to model the linear interdependence of the instantaneous power consumption on the Tx power. An increase in the Tx power results in a linear increase of the instantaneous BS power consumption and vice versa. Nevertheless, even when the Tx power is very low and can be neglected, the proposed linear models ensure some fixed amount of power consumption. Therefore, the proposed linear models contain two components in relations (11) and (12); fixed, which is independent on the Tx power (β_1), and variable ($\beta_2 * P_{Tx}, \beta_2 * P_{Tp}$), which is directly

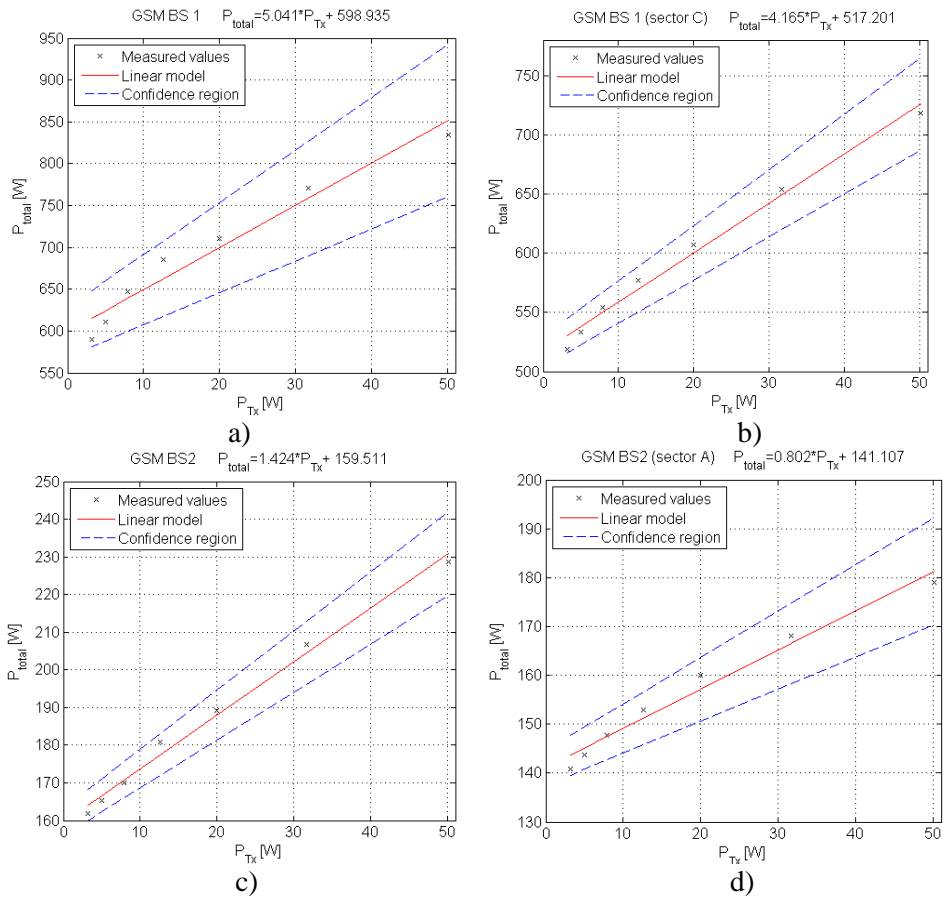


Figure 14. Power consumption model for: a) GSM BS1, b) GSM BS1 (only sector C active), c) GSM BS2 and d) GSM BS2 (only sector A active).

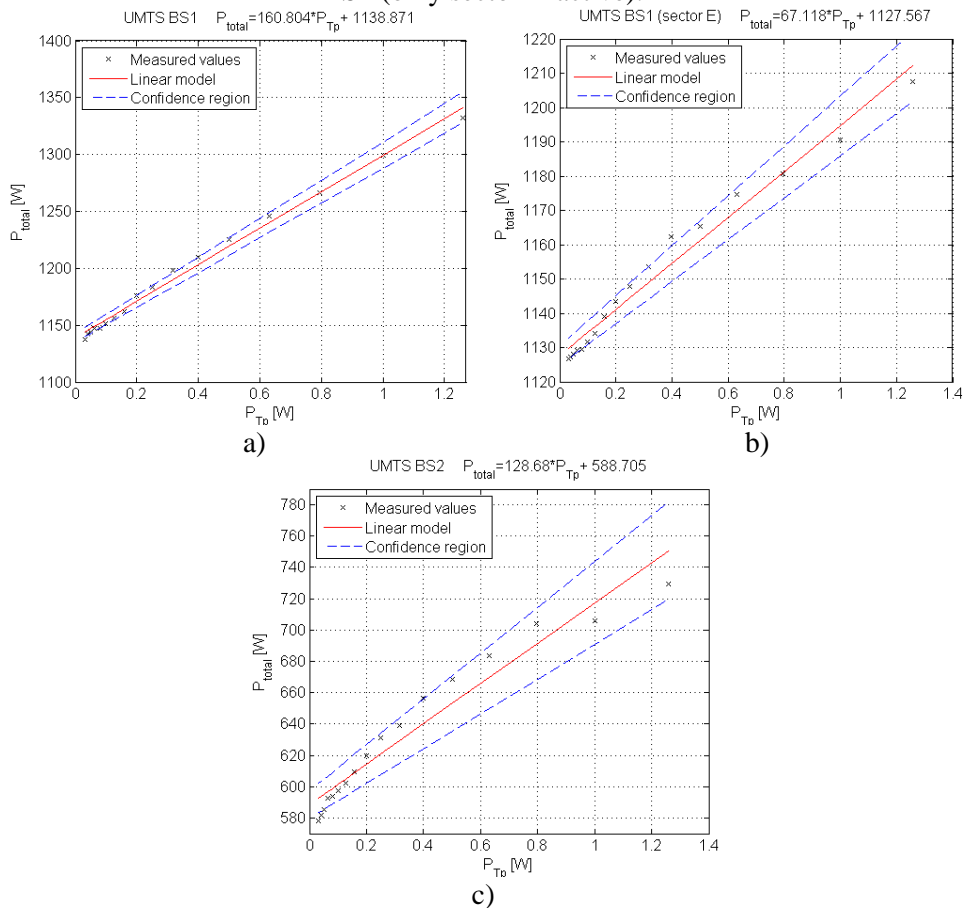


Figure 15. Power consumption model for: a) UMTS BS1, b) UMTS BS1 (only sector D active), and c) UMTS BS2.

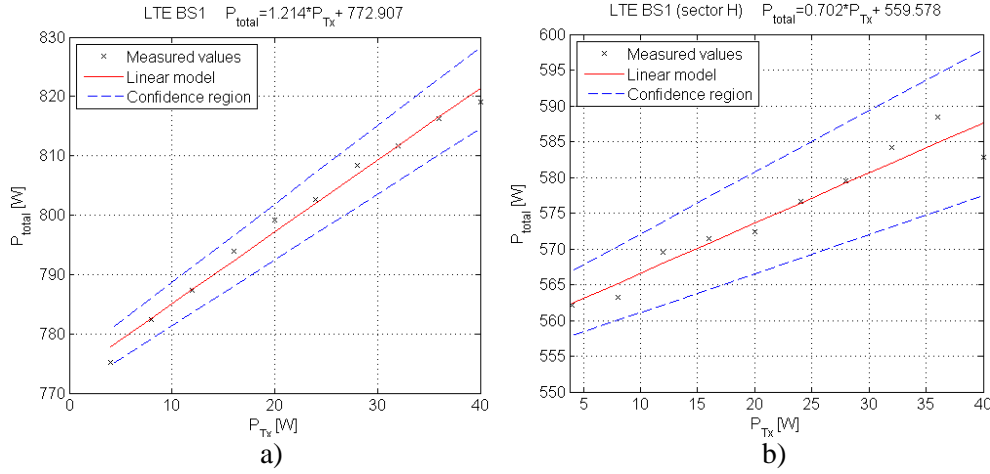


Figure 16. Power consumption model for: a) LTE BS1 and b) LTE BS1 (only sector H active).

Table 5. The developed linear power consumption models for BSs covering a different number of sectors with 2 TRX/sector

BS type	Relative expression	Absolute expression
1 sector with 2TRX/sector		
	β_2 [W], β_1 [W]	β_2, β_1 [W]
GSM BS (older)	$P_{total} = 1.044 * P_{tx_r} + 326.767$	$P_{total} = 2.082 * P_{tx} + 326.767$
GSM BS (newer)	$P_{total} = 0.201 * P_{tx_r} + 70.553$	$P_{total} = 0.401 * P_{tx} + 70.553$
UMTS BS (older)	$P_{total} = 0.845 * P_{tx_r} + 567.567$	$P_{total} = 6.712 * P_{tx} + 567.567$
UMTS BS (newer)	$P_{total} = 0.54 * P_{tx_r} + 196.235$	$P_{total} = 4.289 * P_{tx} + 196.235$
LTE BS (newer)	$P_{total} = 0.162 * P_{tx_r} + 257.634$	$P_{total} = 0.405 * P_{tx} + 257.634$
2 sectors with 2TRX/sector		
	β_2 [W], β_1 [W]	β_2, β_1 [W]
GSM BS (older)	$P_{total} = 1.483 * P_{tx_r} + 544.835$	$P_{total} = 2.959 * P_{tx} + 544.835$
GSM BS (newer)	$P_{total} = 0.513 * P_{tx_r} + 34.457$	$P_{total} = 1.023 * P_{tx} + 34.457$
UMTS BS (older)	$P_{total} = 2 * P_{tx_r} + 1138.9$	$P_{total} = 16.1 * P_{tx} + 1138.9$
UMTS BS (newer)	$P_{total} = 1.08 * P_{tx_r} + 392.47$	$P_{total} = 8.579 * P_{tx} + 392.47$
LTE BS (newer)	$P_{total} = 0.324 * P_{tx_r} + 515.271$	$P_{total} = 0.809 * P_{tx} + 515.271$
3 sectors with 2TRX/sector		
	β_2 [W], β_1 [W]	β_2, β_1 [W]
GSM BS (older)	$P_{total} = 2.527 * P_{tx_r} + 598.935$	$P_{total} = 5.041 * P_{tx} + 598.935$
GSM BS (newer)	$P_{total} = 0.714 * P_{tx_r} + 214.011$	$P_{total} = 1.424 * P_{tx} + 214.011$
UMTS BS (older)	$P_{total} = 2.869 * P_{tx_r} + 1706.4$	$P_{total} = 22.792 * P_{tx} + 1706.4$
UMTS BS (newer)	$P_{total} = 1.62 * P_{tx_r} + 588.705$	$P_{total} = 12.868 * P_{tx} + 588.705$
LTE BS (newer)	$P_{total} = 0.485 * P_{tx_r} + 772.907$	$P_{total} = 1.214 * P_{tx} + 772.907$

proportional to the Tx power.

Generally, there is no major difference in the linearity of models presenting power consumption of complete BSs and BSs having active only those components used for covering a single sector (Figures 14a and b or 14c and d, 15a and b, 16a and b). Each developed linear model corresponds to the specific BS, and it depends on technology, manufacturer, production year, and the hardware configuration of the BS. This confirms that the linear power consumption model can be accepted as a model for expressing the interdependence between instantaneous BS power consumption and Tx power. This is because the proposed approach fairly pursues the results obtained through precise on-site measurements with a significant percentage of confidence. These models can be used with full confidence in future studies focused on improving the energy efficiency of macro BSs having technical characteristics as those presented in Tables 1-3.

6.2. General power consumption models

As previously stated, the models developed in Section 6.1 are precisely related to the BSs with technical characteristics presented in Tables 1-3. In order to have a more general model that is applicable for BSs of

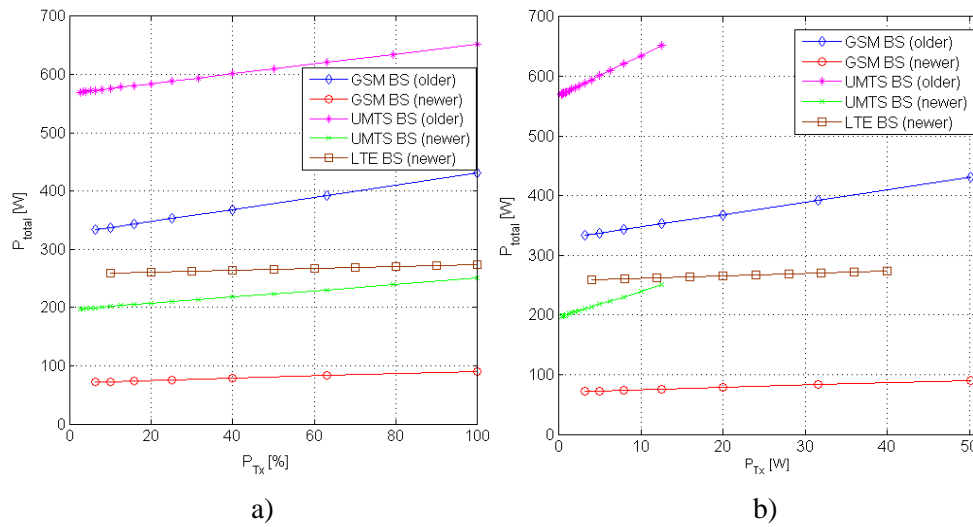


Figure 17. a) Relative and b) absolute expressions of linear models for BSs covering one sector with 2 TRXs/sector.

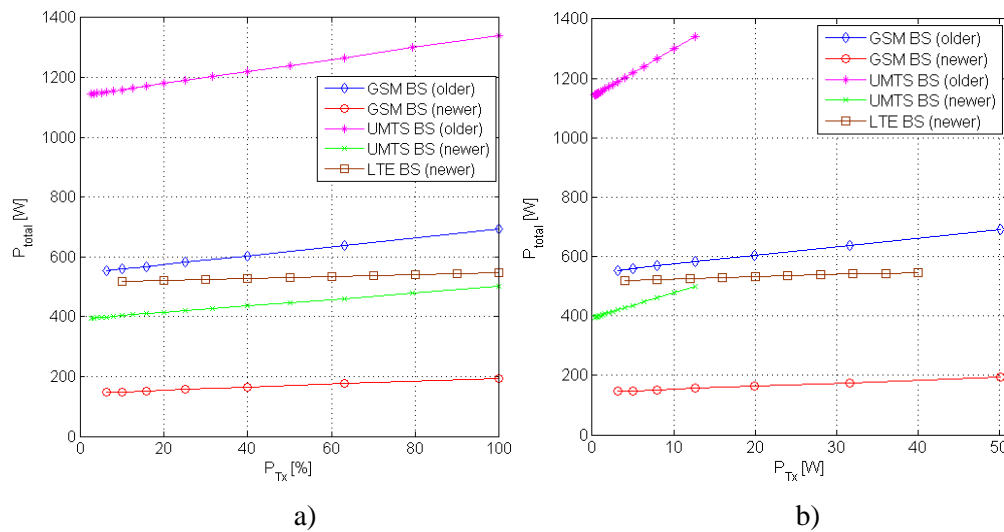


Figure 18. a) Relative and b) absolute expressions of linear models for BSs covering two sectors with 2 TRXs/sector.

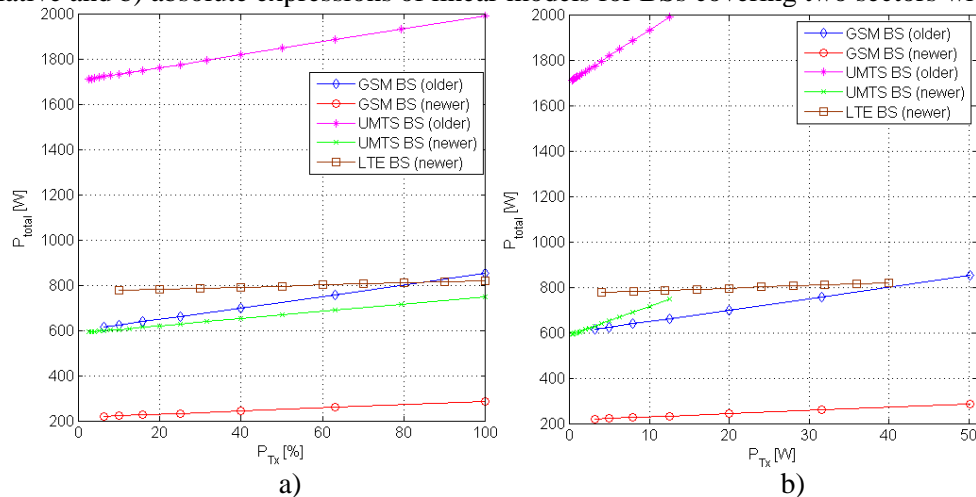


Figure 19. a) Relative and b) absolute expressions of linear models for BSs covering three sectors with 2 TRXs/sector.

known technology and production year, we developed linear power consumption models for each sector covered by the BS rack. The development of such models was based on the interpolation of measured results that we obtain from different operating configurations of the same BS. The developed linear models present interdependence of the consumed and transmitted power in cases when configuration of a single BS rack covers: one sector with two TRXs/sector (Figure 17), two sectors with two TRXs/sector (Figure 18), and three

Table 6. Measured transition time periods of all analyzed macro BSs.

Transitions include all TRXs of BSs			
Analyzed BS	TRXs turning off time period	TRXs turning on time period	Decrease of max. Tx power for one level [s]
	[s]	[s]	
GSM BS1	14	5	9
GSM BS2	21	6	9
UMTS BS1	4	9	8
UMTS BS2	3	4	7
LTE BS	2	2	3
Transitions include TRXs used for covering one sector of BSs			
GSM BS1(sector C)	4	8	6
GSM BS2 (sector A)	3	9	2
UMTS BS1 (sector D)	2	5	4
LTE BS(sector H)	2	2	3

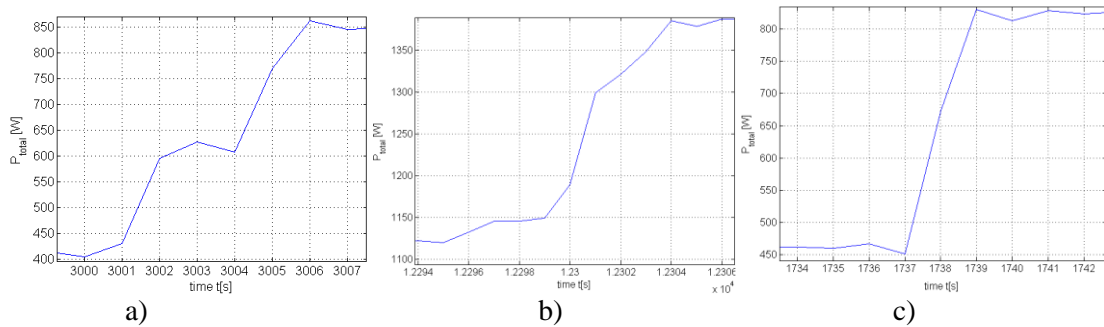


Figure 20. Transient periods in cases of simultaneous powering of all TRXs inside: a) GSM BS1, b) UMTS BS1, c) LTE BS1.

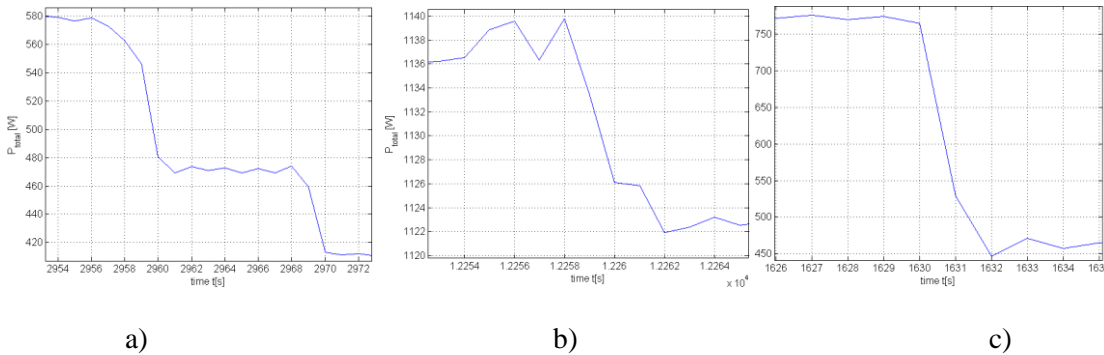


Figure 21. Transient periods in cases of simultaneous shutting down of all TRXs inside: a) GSM BS1, b) UMTS BS1, c) LTE BS1.

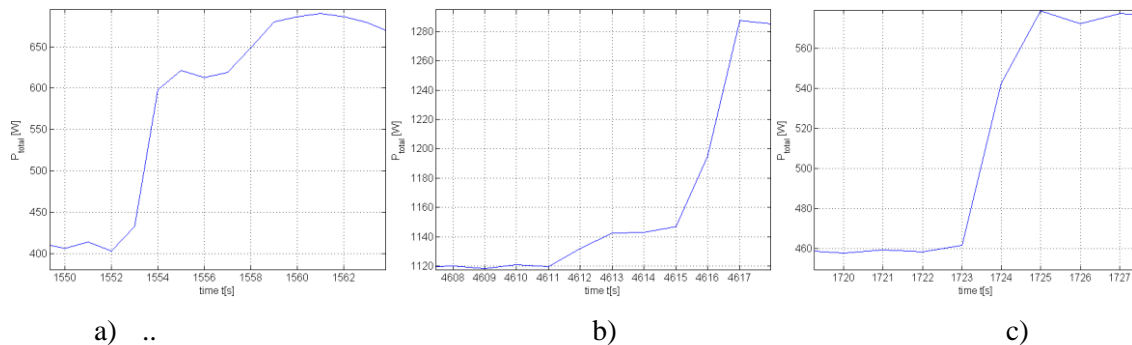


Figure 22. Transient periods in cases of simultaneous powering of TRXs used for covering one sector of: a) GSM BS1, b) UMTS BS1, c) LTE BS1.

sectors with two TRXs/sector (Figure 19). Such configurations are common and basic in many practical implementations.

Mathematical formulation of the developed linear power consumption models for BSs covering different number of sectors with two TRXs/sector are presented in Table 5. It can be noticed that the developed linear power consumption models have been categorized for each BS technology (GSM, UMTS, LTE) in two groups: older and newer. Considering ten years as the minimal estimated lifetime of BS, the group of older BSs is comprised of BS models manufactured before 2005, while BSs produced in the year 2005 and later are categorized as newer BSs. Linear models are developed for the case of relative and absolute expression of interdependence between instantaneous power consumption and Tx power. Absolute expression is equal to those defined with relations (11) and (12), where absolute value of the Tx power is a multiplier in the linear models presented in Table 5. Linear models with a relative expression in Table 5 have a multiplier in the form of coefficients K_{Tx} and K_{Tp} . They express a percentage of the instantaneous Tx power relative to the maximal Tx power. Linear power consumption models with relative expression are defined with next relations:

$$P_{total} = k_{TRX} * (\beta_2 * K_{Tx}) + \beta_1 \quad [W] \quad (13)$$

$$P_{total} = k_{TRX} * (\beta_2 * K_{Tp}) + \beta_1 \quad [W] \quad (14)$$

where coefficients for the GSM and LTE BSs, have been calculated according to:

$$K_{Tx} = \frac{P_{Tx}}{P_{Txmax}} * 100 \quad [%] \quad (15)$$

while the calculation of coefficients for the UMTS BSs is based on the next relation:

$$K_{Tp} = \frac{P_{Tp}}{P_{Tpmax}} * 100 \quad [%] \quad (16)$$

In relations (13) and (14,) constant k_{TRX} defines the multiplication factor, which corresponds to $k_{TRX} = 1, 1.5, 2, 2.5, 3, \dots$ for the number of TRXs/sector equal to $n_{TRX} = 2, 3, 4, 5, 6 \dots$, respectively. Based on the number of active TRXs/sector, coefficient k_{TRX} will have different values. This means that a higher number of active TRXs/sector increases the variable components of the power consumption model. This consequently results in an increase of the total instantaneous power consumption of complete BS.

Figures 17, 18 and 19 depict developed linear models for older and newer types of BSs of different technologies with configurations covering one, two and three sectors with two TRXs/sector ($k_{TRX} = 1$), respectively. Such models can be used as referent models for the presentation of interdependence between consumed and Tx power for BSs of different technologies and production years (generations), having basic configuration with two TRXs/per sector.

The advantage of such an approach is in the possibility of a straightforward extension of the proposed models to more complex configurations containing a different number of TRXs/sector. Such generalization can be done by selecting the appropriate value of multiplication factor k_{TRX} for BSs with the corresponding number of TRXs/sector. It is worth emphasizing that comprehensive generalization is hard to accomplish due to huge differences among hardware characteristics of different BS manufacturers. However, it is reasonable to believe that implemented generalization is performed with high accuracy, since obtained results have been interpolated for BSs of different technologies (2G, 3G, 4G), manufacturers, production years (2000-2012) and configurations (2/3/4/5/6... TRXs/sector).

7. Consumed power in transient periods

7.1 Transient times

With performed continuous measurements, we managed to capture the values of instantaneous BSs power consumption during transient periods. Such periods include changes of instantaneous BS power consumption when:

- all TRXs of a BS change state from on to off and vice versa,
- a BS TRXs used for covering one sector change state from on to off and vice versa,
- maximal Tx power of all TRXs of a BS are decreased simultaneously for one level,

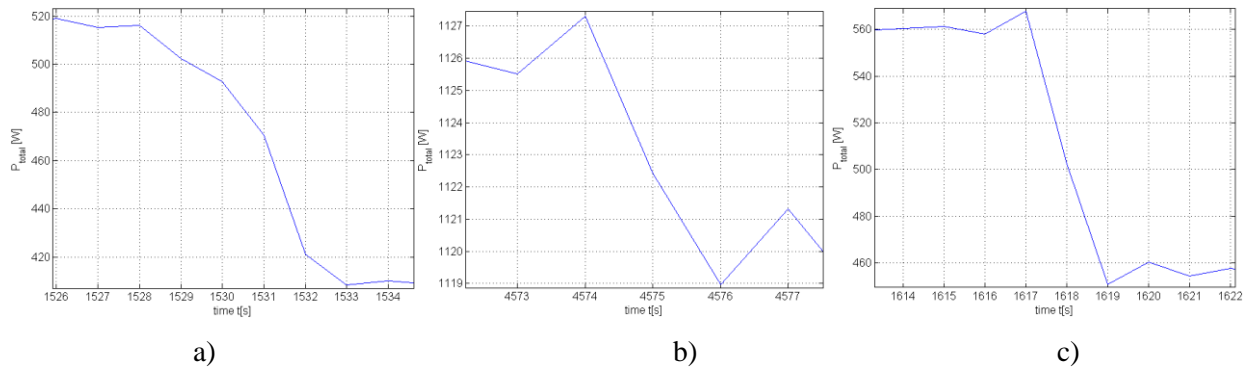


Figure 23. Transient periods in cases of simultaneous turning off TRXs used for covering one sector of: a) GSM BS1, b) UMTS BS1, c) LTE BS1.

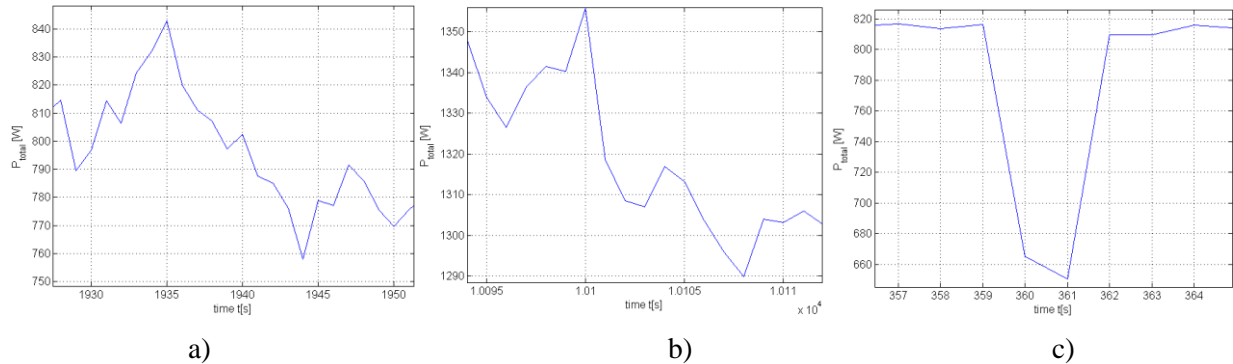


Figure 24. Transient periods in cases of reducing Tx power for one level at: a) GSM BS1, b) UMTS BS1, c) LTE BS1.

Table 7. Power consumption measured when full BSs configuration is active.

Parameters	GSM BS1	GSM BS2	UMTS BS1	UMTS BS2	LTE BS
Max. power consumption at max. Tx power (W)	834.87	228.63	1331.84	729.65	819.06
Static (fixed) power consumption at min. Tx power (W)	590.47	161.83	1137.73	577.85	775.16
Dynamic (variable) power consumption (W)	244,40	67,25	194,11	151,8	43.9
Stand by (fixed) power consumption (W)	410.53	109.33	1125.6	383.36	461.38
Static/Max. power consumption ratio [%]	70.73	70.78	85.43	79.20	94.64
Dynamic/max. power consumption ratio [%]	29.27	29.22	14.57	20.8	5.36
Stand by/Max. power consumption ratio [%]	49.17	47.82	84.51	52.54	56.33
Stand by/static power consumption ratio [%]	69.52	67.55	98.93	66.33	59.52

- maximal Tx power of a BS TRXs used for covering one sector are decreased simultaneously for one level.

It is important to emphasize that all on/off changes and decreases of the Tx power have been initiated remotely, through manual changes performed in the BSs configuration software. Capturing changes of the instantaneous power consumption during transient times is possible since frequency of taking measuring samples is set to one sample per second. The graphs in Figures 20-24 illustrate variations in the instantaneous power during transient times characterized with changes of TRXs on/off state and decreases of the Tx power for one level. In Table 6, exact measured transient times expressed in seconds are listed for all of the analyzed BSs. The upper part of Table 6 indicates transient times measured for changes performed simultaneously on all active TRXs inside each BS rack. The bottom part of Table 6 provides transient times measured when only TRXs used for covering one sector participate in the activity or Tx power changes.

According to the results presented in Table 6, transition times for on/off powering of TRXs or decrease of Tx powers differs slightly among BS technologies and generations. Somewhat longer transition times in the case of TRXs on/off powering can be noticed for older BSs of legacy technologies, such as UMTS and GSM. The macro LTE BS has the lowest transition times due to advanced hardware, and these BSs are the most suitable

Table 8. Power consumption statistics measured with active configuration of BSs used for covering one sector.

Parameters	GSM	GSM	UMTS	LTE
	BS 1 (sector C)	BS 2 (sector A)	BS1 (sector D)	BS (sector H)
Max. power consumption at max. Tx power (W)	718.6	179.03	1207.64	582.77
Static (fixed) power consumption at min. Tx power (W)	518.62	140.92	1126.62	562.17
Dynamic (variable) power consumption (W)	199.98	29.11	81.02	20.6
Stand by (fixed) power consumption (W)	408.77	108.89	1116.6	457.69
Static/Max. power consumption ratio [%]	72.17	78.71	93.29	96.47
Dynamic/Max. power consumption ratio [%]	27.83	21.29	6.71	3.53
Stand by/Max. power consumption ratio [%]	56.88	60.82	92.46	78.54
Stand by/Static power consumption ratio [%]	78.81	77.27	99,11	81.41

for implementation in dynamic resource adaptation environments. Nevertheless, software scaling of the Tx power from one to another level for TRXs covering a single sector can be performed for all technologies in less than six seconds. This also worth's for on/off powering of TRXs used for covering a single sector.

Due to the short duration of transition times, power consumption during these periods can be neglected. This is valuable if the transitions rarely occur during the day. On the other hand, future centralized or distributed algorithms developed for improving network energy-efficiency through the dynamic management of network resources must take into account transition times. During the transition time, service to users can be degraded and this must be predicted with these algorithms.

7.2. Power consumption statistics

As presented in the related work section, most of the research activity dedicated to the energy-efficient management of network resources is based on two approaches: dynamic scaling of the Tx power or off/on adaptation of BS elements (RRUs, TRXs, TRUs) used for covering one or more sectors around BS. Because of that, it is reasonable to investigate the impacts of scaling Tx power and the off/on switching of BS elements on the possible energy savings. Such dynamic scaling and switching can be performed in already installed networks, since network operators through configuration and management software can remotely access each BS. Table 7 presents statistics of BSs power consumption obtained when BSs are active with full configurations (the parameters are indicated in Tables 1-3 and depicted in Figure 1). Similar statistics of power consumption are presented in Table 8, when BSs have only those elements used for covering one sector active, while other elements have been in stand by state (shut down). Hence, stand by state in Tables 7 and 8 means a state in which all or some elements (RRUs, TRXs, TRUs) used to cover all or one sector are remotely turned off, respectively.

From Tables 7 and 8 it can be noticed that an approach based on the off/on switching of elements used for covering one or more sectors is always more favorable for all BSs technologies and generations than an approach based solely on Tx power scaling. This is because a static share in total power consumption is dominant for all BSs technologies (for LTE above 90%, and for GSM and UMTS above 70%). In addition, the stand by share in total BSs power consumption is even lower than the lowest static share (stand by consumption is between 70% and 99% of static consumption). Hence, from an energy saving point of view, putting BSs elements in stand by state (turning off) is better than transmission at lowest Tx power levels. Thus, higher energy savings can be accomplished through the on/off switching approach in comparison with an approach based on Tx power scaling.

Also, it is worth indicating that the share of dynamic components in total (maximal) BS power consumption decreases with the introduction of every new BSs technology (Tables 7 and 8). This means that the dynamic adaptation of Tx power as an approach is more favorable for macro GSM and UMTS BSs, while for LTE BSs this approach cannot bring significant energy savings. This is because reducing the Tx power of macro LTE BS1 to the lowest level can bring maximal energy savings of up to 5 percent. This is significantly lower when compared to maximal savings of up to 30 percent in the case of GSM BSs. Due to more energy-efficient

hardware components, BSs of newer technologies such as LTE have a significant share (95%) of static (fixed) consumption in maximal BS power consumption. In terms of energy savings, it is advisable that macro BSs of all technologies be included in on/off activity management, while Tx power scaling be a dominant approach for the case of macro BS of older technologies such as UMTS and GSM.

8. Conclusions

In this paper, influence of the Tx power and on/off switching of BSs elements on instantaneous power consumption have been analyzed. Through on-site measurements performed on real BSs of the second, third and fourth generations, we detected that due to a decrease of Tx power, instantaneous power consumption of BSs also decreases and vice versa. However, the percentage of this decrease is different for BSs of different generations, production years, and configurations. Obtained measurement results were used for the development of power consumption models by means of linear regression. Models present with significant confidence linear interdependence among instantaneous Tx and consumed power of BSs. In order to have more general models to serve as reference models for BSs of known access technology and oldness, we develop power consumption models per one or more sectors covered with basic BS hardware configuration. Analyses of power consumption statistics indicate that putting in stand by state some or all elements of BSs can bring larger energy savings when compared with transmission at the lowest Tx powers. In terms of energy savings, scaling Tx power as an approach is more favorable for UMTS and GSM BSs, due to a significant share of fixed BS power consumption in total power consumption for LTE BSs. On the other hand, off/on switching of BS elements is always more favorable for all BSs technologies and generations than an approach based solely on Tx power scaling. Also, it is shown that the duration of transient periods needed for remote scaling of Tx power, or changing the activity state of the BS element, is lower in BSs of newer generations.

Our future research activities will be dedicated to developing algorithms for the energy-efficient management of cellular network resources based on Tx power scaling and on/off switching of BSs.

References

- [1] I. Humar, X. Ge and X. Li, "Rethinking Energy Efficiency Models of Cellular Networks with Embodied Energy", *IEEE Network Magazine*, Volume 25, Issue 2, pp. 40-49, March-April 2011., doi: 10.1109/MNET.2011.5730527
- [2] H. Klessig, A. Fehske and G. Fettweis, "Energy Efficiency Gains in Interference-limited Heterogeneous Cellular Mobile Radio Networks with Random Micro Site Deployment", *34th IEEE Sarnoff Symposium*, pp. 1-6, May 2011, doi: 10.1109/SARNOF.2011.5876468
- [3] W. Vereecken, W. Van Heddeghem, D. Colle, M. Pickavet and P. Demeester, "Overall ICT Footprint and Green Communication Technologies", *4th International Symposium on Communications, Control and Signal Processing (ISCCSP)*, pp.1-6, March 2010., doi: 10.1109/ISCCSP.2010.5463327
- [4] Isabelle Gross, Case study: Mitigating ICT-related Carbon Emissions: Using renewable energy to power base stations in Africa's mobile telecommunications sector, 2012.
- [5] O. Blume, H. Eckhardt, S. Klein, E. Kuehn and W. M. Wajda, "Energy Savings in Mobile Networks Based on Adaptation to Traffic Statistics", *Bell Labs Technical Journal*, Volume 15, Issue 2, pp.:77-94, September 2010., doi: 10.1002/bltj.20442
- [6] M. A. Marsan, L. Chiaraviglio, D. Ciullo and M. Meo, "Optimal Energy savings in Cellular Access Networks", *IEEE International Conference on Communications Workshops (ICC Workshops)*, pp.1-5, June 2009., doi: 10.1109/ICCW.2009.5208045
- [7] M. A. Imran, J. Alonso-Rubio, G. Auer, M. Boldi, M. Braglia et al., "Most suitable efficiency metrics and utility functions", *FP 7 EARTH project report, Deliverable D2.4*, January, 2012.
- [8] M. Deruyck, E. Tanghe, W. Joseph and L. Martens, "Modelling and Optimization of Power Consumption in Wireless Access Networks", *Computer Communications*, Volume 34, Issue 17, p.p.:2036.-2046., March 2011., doi: 10.1016/j.comcom.2011.03.008
- [9] T Chen, H. Haesik, Y. Yang: "Energy efficiency metrics for green wireless communications", *Proceedings International Conference on Wireless Communications and Signal Processing (WCSP)*, pp. 1-6, Suzhou, China, October 2010., doi: 10.1109/WCSP.2010.5633634

- [10] F. Richter, A. Fehske and G. Fettweis, "Energy Efficiency Aspects of Base Station Deployment Strategies for Cellular Networks", *IEEE Vehicular Technology Conference (Fall)*, pp. 1-5, 2009., doi: 10.1109/VETEFCF.2009.5379031
- [11] K. Dufkova, M. Popovic, R. Khalili, J. Le Boudec, M. Bjelica and L. Kencl, "Energy Consumption Comparison Between Macro-Micro and Public Femto Deployment in a Plausible LTE Network", *International Conference on Energy-Efficient Computing and Networking*, pp. 67-76, 2011., doi: 10.1145/2318716.2318730
- [12] J. Lorincz, T. Garma and G. Petrovic, "Measurements and Modelling of Base Station Power Consumption under Real Traffic Loads", *Sensors Journal*, Volume 12, Issue 04, pp. 4281-4310, 2012. , doi: 10.3390/s120404281
- [13] G. Auer, O. Blume, V. Giannini, I. Godor, M. Imran, et al., "Energy efficiency analysis of the reference systems, areas of improvements and target breakdown", *FP 7 EARTH project report, Deliverable D2.3*, December, 2010.
- [14] S. Tombaz, K. W. Sung and J. Zander, "Impact of densification on energy efficiency in wireless access networks", *IEEE Globecom Workshops (GC Wkshps)*, pp. 57-62, December 2012, doi: 10.1109/GLOCOMW.2012.6477544
- [15] A. Mukherjee, S. Bhattacharjee, S. Pal and D. De, "Femtocell based green power consumption methods for mobile network", *Computer Networks Journal*, Volume 57, Issue 01, pp. 162-178, January 2013., doi: 10.1016/j.comnet.2012.09.007
- [16] L. G. Hevizi and I. Gódor, "Power savings in mobile networks by dynamic base station sectorization", *IEEE 22nd International Symposium on Personal Indoor and Mobile Radio Communications (PIMRC)*, pp. 2415-2417, September 2011, doi: 10.1109/PIMRC.2011.6139954
- [17] M. Nahas, S. Abdul-Nabi, L. Bouchnak and F. Sabeh, "Reducing Energy Consumption in Cellular Networks by Adjusting Transmitted Power of Base Stations", *Symposium on Broadband Networks and Fast Internet (RELABIRA)*, pp. 39-44, May 2012., doi: 10.1109/RELABIRA.2012.6235090
- [18] J. Lorincz, A. Capone, D. Begusic, "Optimized Network Management for Energy Savings of Wireless Access Networks", *Computer Networks Journal*, Vol. 55, No.: 3, 514 – 540, 2011, doi: 10.1016/j.comnet.2010.09.013
- [19] J. Lorincz, A. Capone, D. Begusic, "Impact of Service Rates and Base Station Switching Granularity on Energy Consumption of Cellular Networks", *EURASIP Journal on Wireless Communications and Networking*, 2012:(342), 2012, doi: 10.1186/1687-1499-2012-342
- [20] X. Weng, D. Cao, and Z. Niu, "Energy-efficient cellular network planning under insufficient cell zooming", *73rd Vehicular Technology Conference (VTC Spring) IEEE*, pp. 1-5, May 2011, doi: 10.1109/VETECS.2011.5956699
- [21] A. Conte, A. Feki, L. Chiaraviglio, D. Ciullo, M. Meo and M. A. Marsan, "Cell wilting and blossoming for energy efficiency". *Wireless Communications, IEEE*, Volume 18, Issue 5, October 2011, pp. 50-57, doi: 10.1109/MWC.2011.6056692
- [22] S. Han, C. Yang, G. Wang and M. Lei, "On the energy efficiency of base station sleeping with multicell cooperative transmission". *IEEE 22nd International Symposium on Personal Indoor and Mobile Radio Communications (PIMRC)*, pp. 1536-1540, September 2011, doi: 10.1109/PIMRC.2011.6139761
- [23] T. Han and N. Ansari, "On greening cellular networks via multicell cooperation", *Wireless Communications, IEEE*, Volume 20, Issue 1, pp. 82-89, February 2013, doi: 10.1109/MWC.2013.6472203
- [24] M. F. Hossain, K. S. Munasinghe and A. Jamalipour, "On the Energy Efficiency of Self-Organizing LTE Cellular Access Networks", *IEEE GLOBECOM 2012*, pp.: 5314 – 5319, 2012, 10.1109/GLOCOM.2012.6503965
- [25] M. Sreasser, D. Martin, "Remote Radio Installation", *White paper*, HuBER+SuHnER AG, 2010
- [26] G. Kutner, M., "Applied Linear Regression Models", *McGraw Hill*: New York, USA, 2004.
- [27] Joint Committee: Evaluation of Measurement Data—An Introduction to the Guide to the Expression of Uncertainty in Measurement. Available online: <http://www.bipm.org>
- [28] Stephen Wilkus, "Power consumption trends in wireless networks", *e-Energy Conference, Alcatel-Lucent*, June 2011